

SYNTHESIS OF DOPAMINE FUNCTIONALIZED SILVER NANOPARTICLES TOGETHER  
WITH POSSIBLE INTERACTIONS BETWEEN SILVER AND DOPAMINE HAVING  
DIFFERENT OXIDATION FORMS

A THESIS SUBMITTED TO  
THE GRADUATE SCHOOL OF NATURAL AND APPLIED SCIENCES  
OF  
MIDDLE EAST TECHNICAL UNIVERSITY

BY

ELİF KANBERTAY

IN PARTIAL FULFILLMENT OF THE REQUIREMENTS  
FOR  
THE DEGREE OF MASTER OF SCIENCE  
IN  
CHEMISTRY

FEBRUARY 2013

Approval of the Thesis:

SYNTHESIS OF DOPAMINE FUNCTIONALIZED SILVER NANOPARTICLES TOGETHER  
WITH POSSIBLE INTERACTIONS BETWEEN SILVER AND DOPAMINE HAVING  
DIFFERENT OXIDATION FORMS

submitted by **ELİF KANBERTAY** in partial fulfillment of the requirements for the degree of **Master of Science in Chemistry Department, Middle East Technical University** by,

Prof. Dr. Canan Özgen  
Dean, Graduate School of **Natural and Applied Sciences**

\_\_\_\_\_

Prof. Dr. İlker Özkan  
Head of Department, **Chemistry**

\_\_\_\_\_

Prof. Dr. Mürvet Volkan  
Supervisor, **Chemistry Dept., METU**

\_\_\_\_\_

**Examining Committee Members:**

Prof. Dr. Ahmet M. Önal  
Chemistry Dept., METU

\_\_\_\_\_

Prof. Dr. Mürvet Volkan  
Chemistry Dept., METU

\_\_\_\_\_

Prof. Dr. Ceyhan Kayran  
Chemistry Dept., METU

\_\_\_\_\_

Doç. Dr. Nursen Çoruh  
Chemistry Dept., METU

\_\_\_\_\_

Doç. Dr. Atilla Cihaner  
Chemical Engineering and Applied Chemistry Dept.,  
Atılım University

\_\_\_\_\_

**Date:**

18.02.2013

**I hereby declare that all information in this document has been obtained and presented in accordance with academic rules and ethical conduct. I also declare that, as required by these rules and conduct, I have fully cited and referenced all material and results that are not original to this work.**

Name, Last name : Elif Kanbertay

Signature :

## ABSTRACT

### **SYNTHESIS OF DOPAMINE FUNCTIONALIZED SILVER NANOPARTICLES TOGETHER WITH POSSIBLE INTERACTIONS BETWEEN SILVER AND DOPAMINE HAVING DIFFERENT OXIDATION FORMS**

Kanbertay, Elif  
M.Sc., Department of Chemistry  
Supervisor: Prof. Dr. Mürvet Volkan

February 2013, 40 pages

Dopamine is a neurotransmitter found in central nerve system which has a vital role for human health. Dopamine oxidation in body is an important issue since it may form reactive metabolites which can be toxic to the cell. Surface-enhanced Raman scattering (SERS) is currently recognized as one of the most sensitive spectroscopic tools, which can be exploited for ultrasensitive chemical and biological detection, addition to providing structural information on the systems of interest. SERS of dopamine displays three strong bands at 1269, 1331 and 1479  $\text{cm}^{-1}$ . These bands are the signature of dopamine molecule. The most intense band at 1479  $\text{cm}^{-1}$  is contributed mainly from stretching of the carbon-carbon bond to which the oxygens are attached. A bidentate silver-dopamine complex or in general bidentate metal-dopamine complex formation is required for the SERS detection of dopamine and other catecholamines. In other words, for acquiring the characteristic dopamine SERS signature, both of the catechol oxygens should take a part in the adsorption of dopamine to the silver metal surface which is used as a SERS substrate. Therefore, the reactivity of different oxidation forms of dopamine for the formation of bidentate silver-dopamine complex was investigated by obtaining their SERS spectra and following the characteristic C-C ring vibration at 1479  $\text{cm}^{-1}$ . Dopamine oxidation was carried out electrochemically, utilizing platinum and silver electrodes as working electrode. Oxidation products formed were identified with UV-vis Spectrometer. Also, silver metal ions were used to oxidize dopamine, leading to formation silver nanoparticles. Dopamine functionalized silver nanoparticles were characterized by Scanning Electron Microscope, Transmission Electron Microscope, UV-vis Spectrometer. Surface-enhanced Raman spectra of polydopamine on the surface of synthesized silver nanoparticles and the electrodeposited dopamine on the porous surface of silver electrode were also obtained.

**Keywords:** Dopamine, silver nanoparticles, electrochemical oxidation

## ÖZ

### DOPAMİN GRUPLARI İÇEREN GÜMÜŞ NANOPARÇACIKLARIN HAZIRLANMASI VE DOPAMİNİN FARKLI OKSİTLENME BASAMAKLARININ GÜMÜŞ İLE ETKİLEŞİMİ

Kanbertay, Elif  
Yüksek Lisans, Kimya Bölümü  
Tez Yöneticisi: Prof. Dr. Mürvet Volkan

Şubat 2013, 40 sayfa

Dopamin, merkezi sinir sisteminde bulunan ve insan sağlığı için önemli rol oynayan bir nörotransmitterdir. Dopaminin vücut içindeki oksidasyonu da hücre için toksik olabilecek metabolitler oluşturabileceğinden büyük önem taşımaktadır. İlgili alan sistemler hakkında sağladığı yapısal bilginin yanı sıra, Yüzye Güçlendirilmiş Raman Spektroskopisi (YGRS) ultra hassas kimyasal ve biyolojik taramalarda kullanılan en hassas spektroskopik araçlardan biri olarak kabul edilmiştir. Dopamin, YGRS'de 1269, 1331 ve 1479  $\text{cm}^{-1}$ 'de olmak üzere üç adet şiddetli bant vermektedir. Bu bantlar dopamin molekülünün imzası olarak nitelendirilebilir. 1479  $\text{cm}^{-1}$ 'deki en büyük bant, oksijenlerin bağlı olduğu karbon-karbon bağının esnemesinden kaynaklanmaktadır. Dopaminin veya diğer katekolaminlerin YGRS ile belirlenebilmesi için iki dişli bir gümüş-dopamin kompleksinin veya genel olarak iki dişli metal-dopamin kompleksinin oluşması gerekmektedir. Başka bir deyişle, dopamine özgün YGRS sinyallerinin gözlemlenebilmesi için dopaminin YGRS substratı olarak kullanılan gümüş metal yüzeyine tutunmasında katekol oksijenlerinin rol alması gerekir. Böylece, dopaminin farklı oksidasyon durumlarının iki dişli gümüş-dopamin komplekslerinin oluşumunda tepkime verme istekleri, YGRS spektrumları ve 1479  $\text{cm}^{-1}$ 'deki karakteristik halka C-C bağı titreşim sinyali kullanılarak anlaşılabilir. Dopaminin oksidasyonu, platin ve gümüş elektrodlar kullanılarak elektrokimyasal olarak gerçekleştirilmiştir. Oluşan oksidasyon ürünleri Ultraviyole ve görünür bölge Spektrometresi ile tanımlanmıştır. Ayrıca, gümüş metal iyonları da dopamini yükseltmek için kullanılmış ve gümüş nanoparçacıkların oluşmasına yol açmıştır. Dopaminle işlevselleştirilmiş gümüş nanoparçacıkları Taramalı Elektron Mikroskopu, Geçirimli Elektron Mikroskopu ve Ultraviyole ve görünür bölge Spektrometresi ile karakterize edilmiştir. Sentezlenen gümüş nano parçacıkların yüzeyindeki dopaminin ve gümüş elektrodun gözenekli yüzeyinde elektrokimyasal tepkime sonucu biriken dopaminin YGRS spektrumları elde edilmiştir.

**Anahtar Kelimeler:** Dopamin, gümüş nanoparçacık, elektrokimyasal yükseltgenme

To My Family,

## ACKNOWLEDGEMENTS

I would like to thank sincerely to my supervisor Prof. Dr. Mürvet Volkan for her valuable guidance, patience, understanding and encouragement throughout this thesis study.

I am grateful to Prof. Dr. Ahmet Önal for his precious contribution, help and support.

I owe special thanks to METU Central Laboratory, especially Prof. Dr Hayrettin Yücel and Prof. Dr. Necati Özkan for their endless patience and encouragement. Things have been much easier thanks to their understanding. Also, I would like to express my gratitude to my colleagues Binnur Özkan and Aysel Kızıltay for their support.

I would like to thank my group mates Ceren Uzun, Dilek Ünal, Ufuk Özgen and Yeliz Akpınar for their friendship and help. They made easier and fun to work at laboratory.

My special thanks go to Gülfem Aygar, Melike Karakuş, Tuğba Endoğan and Tuğba Nur Alp Aslan for their love, friendship, support and million laughs we had. They were there whenever I need. We had the best time together, I love you so much girls.

My deepest thanks go to my family Mesut Kanbertay, Sebahat Kanbertay and Ozan Kanbertay. I couldn't succeed without their love, trust, encouragement and support.

## TABLE OF CONTENTS

ABSTRACT .....	v
ACKNOWLEDGEMENTS .....	viii
TABLE OF CONTENTS .....	ix
LIST OF FIGURES .....	xi
LIST OF TABLES .....	xii
LIST OF ABBREVIATIONS .....	xiii
CHAPTER 1 .....	1
INTRODUCTION .....	1
1.1 Nanotechnology .....	1
1.2 Nanomaterials.....	1
1.3 Silver Nanoparticles and Their Properties .....	1
1.3.1 Synthesis of Silver Nanoparticles.....	2
1.3.1.1 Chemical Reduction Method.....	2
1.4 Dopamine .....	2
1.4.1 Oxidation of Dopamine .....	3
1.4.2 Polymerization of Dopamine.....	4
1.5 Electrochemistry.....	5
1.5.1 Controlled Potential Coulometry.....	6
1.5.2 Cyclic Voltammetry .....	6
1.6 Raman Spectroscopy .....	6
1.6.1 Surface Enhanced Raman Spectroscopy .....	6
1.7 SERS Determination of Dopamine .....	7
1.8 Aim of study.....	7
CHAPTER 2 .....	9
EXPERIMENTAL.....	9
2.1 Chemical Reagents.....	9
2.2 Instrumentation.....	9
2.2.1 Field Emission Scanning Electron Microscope (FE-SEM) .....	9
2.2.2 Transmission Electron Microscope (TEM) .....	9
2.2.3 UV-vis Spectrophotometer .....	10
2.2.4 Raman Spectroscopy .....	10
2.2.5 Electrochemical Measurements .....	10
2.3 Preparation of Silver Colloid.....	10
2.4 Preparation of Surface Modified Silver Nanoparticles with Dopamine .....	11
2.5 Electrochemical Oxidation of Dopamine .....	11
2.5.1 Oxidation of Dopamine by Platinum Electrode.....	12
2.5.1.2 Oxidation of Dopamine in Neutral Medium.....	12



2.5.1.3 Oxidation of Dopamine in Acidic Medium.....	13
2.5.2 Oxidation of Dopamine by Silver Electrode .....	14
2.5.2.1 Oxidation of Dopamine in Neutral Medium.....	14
2.5.2.2 Oxidation of Dopamine Acidic Medium .....	15
2.6 Raman Spectroscopic Analysis .....	16
CHAPTER 3 .....	18
RESULTS AND DISCUSSION .....	18
3.1 Electrochemical Oxidation of Dopamine on Platinum Electrode.....	18
3.1.1 Oxidation of Dopamine in Neutral Medium.....	18
3.2 Electrochemical Oxidation of Dopamine on Silver Electrode.....	21
3.2.1 Oxidation of Dopamine in Neutral Medium.....	21
3.2.2 Oxidation of Dopamine in Acidic Medium .....	22
3.3 Preparation of Dopamine Functionalized Silver Nanoparticles.....	25
3.3 Raman Spectroscopy Studies .....	34
CHAPTER 4 .....	37
CONCLUSION.....	37
REFERENCES.....	38

## LIST OF FIGURES

Figure 1 Dopamine molecule (Bisaglia <i>et al.</i> , 2007).....	3
Figure 2 Oxidation of dopamine (Stokes <i>et al.</i> , 1999) .....	4
Figure 3 Proposed PDA structures (Dreyer <i>et al.</i> , 2012).....	5
Figure 4 Oxidative polymerization of dopamine showing two of the possible structures formed (Postma <i>et al.</i> , 2009) .....	5
Figure 5 SEM image of synthesized Ag colloid.....	11
Figure 6 Cyclic voltammogram of pH 6 PBS, at Pt electrode (from -0.2 V to 0.8 V) .....	12
Figure 7 Cyclic voltammogram of DA, in pH 6 PBS, at Pt electrode (from -0.2 V to 0.8 V) .....	13
Figure 8 Cyclic voltammogram of pH 3 citrate buffer, at Pt electrode (from -0.2 V to 0.8 V).....	13
Figure 9 Cyclic voltammogram of DA, in pH 3 citrate buffer, at Pt electrode (from -0.2 V to 0.8 V)..	14
Figure 10 Cyclic voltammogram of pH 7 KClO <sub>4</sub> , Ag electrode (from -0.1 V to 0.3 V).....	15
Figure 11 Cyclic voltammogram of DA, in pH 7 KClO <sub>4</sub> , at Ag electrode (from -0.1 V to 0.3 V) .....	15
Figure 12 Cyclic voltammogram of pH 3 KClO <sub>4</sub> , at Ag electrode (from -0.1 V to 0.3 V).....	16
Figure 13 Cyclic voltammogram of DA, in pH 3 KClO <sub>4</sub> , at Ag electrode (from -0.1 V to 0.3 V) .....	16
Figure 14 UV-vis spectrum of oxidation product on Pt electrode, in pH 6 PBS, at 0.6 V .....	19
Figure 15 Aminochrome(dopaminechrome) formation mechanism (Bisaglia <i>et al.</i> , 2007).....	19
Figure 16 UV-vis spectra of DA oxidation products on Pt electrode, in pH 3 citrate buffer, at 0.6 V.	20
Figure 17 UV-vis spectra of DA oxidation products on Pt electrode, in pH 3 citrate buffer, at 0.6 V.	20
Figure 18 Polymerization of dopamine (Jiang <i>et al.</i> , 2011) .....	21
Figure 19 UV-vis spectra of DA oxidation products on Ag electrode, in pH 7 KClO <sub>4</sub> , at 0.2 V .....	22
Figure 20 UV-vis spectra of DA oxidation products on Ag electrode, in pH 7 KClO <sub>4</sub> , at 0.2 V .....	22
Figure 21 UV-vis spectra of DA oxidation products on Ag electrode, in pH 3 KClO <sub>4</sub> , at 0.25 V .....	23
Figure 22 UV-vis spectra of DA oxidation products on Ag electrode, in pH 3 KClO <sub>4</sub> , at 0.25 V .....	23
Figure 23 UV-vis spectra of DA oxidation products on Ag electrode, in pH 3 KClO <sub>4</sub> , at 0.25 V .....	24
Figure 24 UV-vis spectra of DA oxidation products on Ag electrode, in pH 3 KClO <sub>4</sub> , at 0.20 V .....	24
Figure 25 The appearance of the DA functionalized Ag NPs synthesized at $\mu\text{M}$ concentration levels of the precursors, as stated in Table 1.....	26
Figure 26 TEM image of Ag NPs formed in experiment 3 in Table 1 (80 $\mu\text{M}$ AgNO <sub>3</sub> , 10 $\mu\text{M}$ DA & 1 mM NaOH) .....	27
Figure 27 TEM image of Ag NPs formed in experiment 9 in Table 1 (80 $\mu\text{M}$ AgNO <sub>3</sub> , 40 $\mu\text{M}$ DA & 1 mM NaOH) .....	27
Figure 28 UV-vis spectra of Ag NPs synthesized with different amounts of AgNO <sub>3</sub> , DA and NaOH	28
Figure 29 Polymerized DA .....	29
Figure 30 DA functionalized Ag NPs dispersions synthesized at mM concentration levels of the precursors, as stated in Table 3 .....	29
Figure 31 SEM image of Ag NPs, experiment 14 in Table 3 (8mM AgNO <sub>3</sub> , 1 mM DA & 25 $\mu\text{M}$ NaOH).....	30
Figure 32 SEM image of Ag NPs, experiment 16 in Table 3 (8mM AgNO <sub>3</sub> , 2 mM DA & 25 $\mu\text{M}$ NaOH).....	31
Figure 33 SEM image of Ag NPs, experiment 15 in Table 3 (8mM AgNO <sub>3</sub> , 1 mM DA & 10 $\mu\text{M}$ NaOH).....	32
Figure 34 UV-vis spectra of experiments 19 & 20.....	33
Figure 35 UV-vis spectra of experiments 21, 22 & 23.....	34
Figure 36 Surface-enhanced Raman spectrum of 10 <sup>-3</sup> M DA solution.....	35
Figure 37 Raman spectrum of polydopamine on the surface of synthesized Ag NPs .....	35
Figure 38 Surface-enhanced Raman spectrum of silver electrode surface after electrolysis of dopamine in pH 7 KClO <sub>4</sub> .....	36

## LIST OF TABLES

Table 1 The summary of the experimental conditions in terms of the concentrations of the precursors (at micromolar level) and the base .....	25
Table 2 The summary of the experimental conditions in terms of the concentrations of the precursors (at millimolar level) and the base .....	28
Table 3 The summary of the experimental conditions in terms of the concentrations of the precursors (at millimolar level) and the base (low concentrations of NaOH).....	29
Table 4 The summary of the experimental conditions in terms of the concentrations of the precursors (at millimolar level), without NaOH .....	32
Table 5 The summary of the experimental conditions in terms of the concentrations of the precursors (at millimolar level), without NaOH .....	33
Table 6 Raman bands of DA ( $\text{cm}^{-1}$ ) (Lee <i>et.al</i> , 1988).....	34

## LIST OF ABBREVIATIONS

AC	Aminochrome
Ag	Silver
CV	Cyclic Voltammetry
DA	Dopamine
DC	Dopamine-chrome
DQ	Dopamine-quinone
NP	Nanoparticle
PBS	Phosphate buffered saline
PDA	Polydopamine
Pt	Platinum
UV-vis	Ultraviolet- visible
SEM	Scanning Electron Microscope
SERS	Surface-enhanced Raman Spectroscopy
TEM	Transmission Electron Microscope

## CHAPTER 1

### INTRODUCTION

#### 1.1 Nanotechnology

A nanometer refers to the length of  $10^{-9}$  m. Nanotechnology deals with nanoscale sized structures and materials. It basically covers the design, production, modification and application of nanomaterials and also investigation of the relation among their dimensions and physical properties (Cao, 2004). It is a multidisciplinary area which concerns various branches of science such as engineering, biology, physics and chemistry (Ferrari, 2005). It is rapidly developing and the need for nanotechnology will continue to increase constantly. Improvements on nanoscience will have significant effects on fields such as materials, electronics, medicine, environment and military (Mnyusiwalla *et al.*, 2003).

#### 1.2 Nanomaterials

Nanomaterials can be defined at the 1–100 nm scale. Their small size is what makes them functional. There are a wide variety of nanomaterials with various structure, size, shape and composition (Wang, 2005). They have unique physical, chemical, electrical, mechanical, magnetic and imaging properties due to their small size. Advances in nanotechnology are directly related to development of synthesis of various and specific nanomaterials. Recently, a variety of nanostructured materials with highly controlled and interesting properties have been produced.

By controlling structure at the nanoscale dimensions, one can control and alter the properties of nanostructures in accordance with the needs of a specific application (West & Halas, 2003).

#### 1.3 Silver Nanoparticles and Their Properties

Silver nanoparticles possess novel optical, electrical and thermal properties. Owing to that, they have various applications in different areas such as electronics, optics and catalysis. Its optical properties make it useful for molecular diagnostic and photonic instruments. It has been recently and popularly used as antibacterial/antifungal agents in biotechnology and bioengineering, textile engineering, coating industry and water treatment.

Collective oscillations of conduction electrons constitute the unique optical properties of silver nanoparticles. When they are excited by electromagnetic radiation, are termed surface plasmon polariton resonances (Chumanov & Evanoff, 2005). Because of surface plasmon resonance, silver nanoparticles exhibit strong bands in the visible region. Consequently, UV-visible absorption spectra are very sensitive to particle size and aggregation condition (Song *et al.*, 2009).

Silver nanoparticles are widely used to obtain Surface Enhanced Raman Scattering. Kniepp *et al.* and Brus *et al.* have proved the fact that not all particles are Surface-enhanced Raman active.

However, their aggregation can cause the enhancement through the formation of “hot spots” (an intense plasmon resonance that exists between two particles in close proximity). Xa *et al.* and Van Duyne *et al.* have indicated that the enhancement factors for a “hot spot” can be up to  $10^{13}$  to  $10^{14}$ . This effect may be the result of combined optical and electromagnetic mechanisms (Glaspell *et al.*, 2005).

### **1.3.1 Synthesis of Silver Nanoparticles**

There are numerous methods to produce silver nanoparticles such as chemical reduction, thermal decomposition, laser ablation, microwave irradiation, electrochemical and sonochemical synthesis (Starowicz *et al.*, 2006).

#### **1.3.1.1 Chemical Reduction Method**

Chemical reduction method is most commonly employed for the synthesis of silver nanoparticles which utilizes a reducing agent such as  $\text{NaBH}_4$ , citrate, ascorbate and saccharide to reduce a silver salt solution. Also, stabilizer agents are used to avoid the aggregation of silver nanoparticles. Particle size, shape and aggregation of silver nanoparticles depend on different variables, such as reducing agent, initial silver salt concentration, reducing agent/silver salt molar ratio, stabilizer concentration, solution temperature and reaction time (Song *et al.*, 2009). In the traditional method, sodium citrate is used as both the reducer and stabilizer (Lee & Meisel, 1982). However, use of citrate (a weak reductant) results in nanoparticles having a wide size distribution. When a strong reductant such as sodium borohydride is used, small particles are produced; but generation of larger particles can't be controlled (Panacek, 2006).

Chemical reduction technique has advantages of generating nanoparticles with the desirable size and shape and without aggregation, high yield, low preparation cost (Kim *et al.*, 2004).

## **1.4 Dopamine**

Neurotransmitters are regarded as chemical messengers who conduct information throughout body and brain. They carry and tune the signals between nerve cells and other cell, mediate signal states between cells in the nervous system (Entschladen *et al.*, 2002).

Dopamine is a neurotransmitter which serves a variety of functions throughout the nervous, renal, hormonal, and cardiovascular systems. It is generated in various parts of central and peripheral nervous system (Shervedani & Alinajafi –Najafabadi, 2011) (Corona-Avendano *et al.*, 2007).

Decrease of dopamine level in human body may lead to brain diseases such as Parkinson's disease, Schizophrenia, etc. (Selvaraju & Ramaraj, 2003). Chemical structure of dopamine is given in Figure 1.

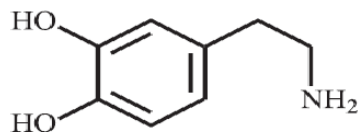


**Figure 1** Dopamine molecule (Bisaglia *et al.*, 2007).

#### 1.4.1 Oxidation of Dopamine

DA has the ability to produce harmful reactive oxygen species such as hydrogen peroxide, superoxide radical, and hydroxyl radical. This may occur through the normal metabolism of DA which is accomplished, in part, by the enzyme monoamine oxidase and produces hydrogen peroxide. From this reaction alone, dopaminergic neurons are exposed to oxidative stress.

DA can form reactive metabolites which have been known to be directly toxic to the cell or play role pathological processes associated with neurodegeneration. DA can be oxidized to a reactive quinone molecule due to the unstable nature of the catechol ring (vicinal hydroxyls on an aromatic ring) (Figure 2). This quinone formation may occur spontaneously, is accelerated by transition metal ions or can be catalyzed by a number of different enzymes and other chemicals (Stokes *et al.*, 1999). Peroxynitrite, peroxidase/H<sub>2</sub>O<sub>2</sub> system, tyrosinase enzyme are most widely used to oxidize dopamine (Kerry & Rice-Evans, 1999) (Napolitano *et al.*, 1995).

Dopamine oxidation is also achieved by electrochemical techniques. Countless research has been done investigating electrochemical oxidation of dopamine for years. Different types of bare and modified electrodes have been employed as well as various oxidative conditions.

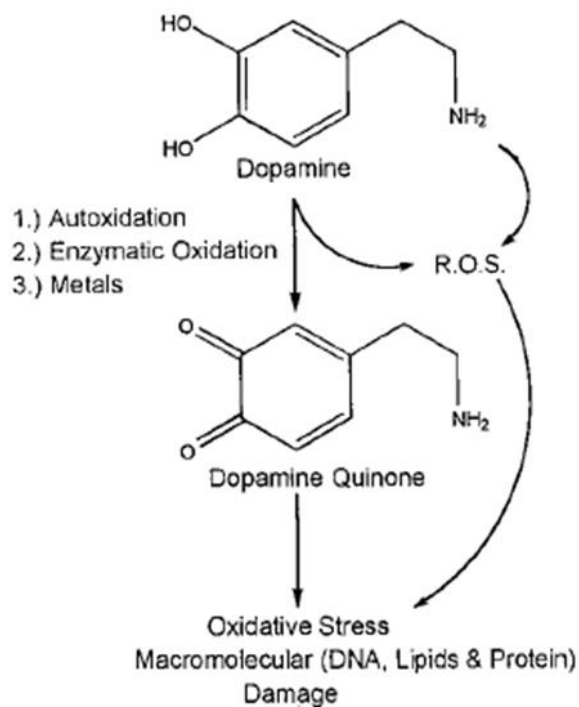


**Figure 2** Oxidation of dopamine (Stokes *et al.*, 1999)

#### 1.4.2 Polymerization of Dopamine

Recently, interest in polydopamine as a surface modification agent has grown in many areas including chemistry, biotechnology, electrochemistry and nanotechnology.

Molecular structure of polydopamine has not been fully understood yet. There are different opinions suggesting different formation mechanisms. Path (I) was suggested by Messersmith *et al.* in which, oxidized and cyclized dopamine monomers were covalently joined via aryl-aryl linkages (Figure 3). Postma *et al.* proposed a similar structure with two possibilities (Figure 4). Other covalent models (II/III) have also been proposed. (IV) is a covalently bound oligomer stack through  $\pi$ - $\pi$  and other noncovalent interactions to form larger supramolecular complex. (Messersmith *et al.*, 2007).



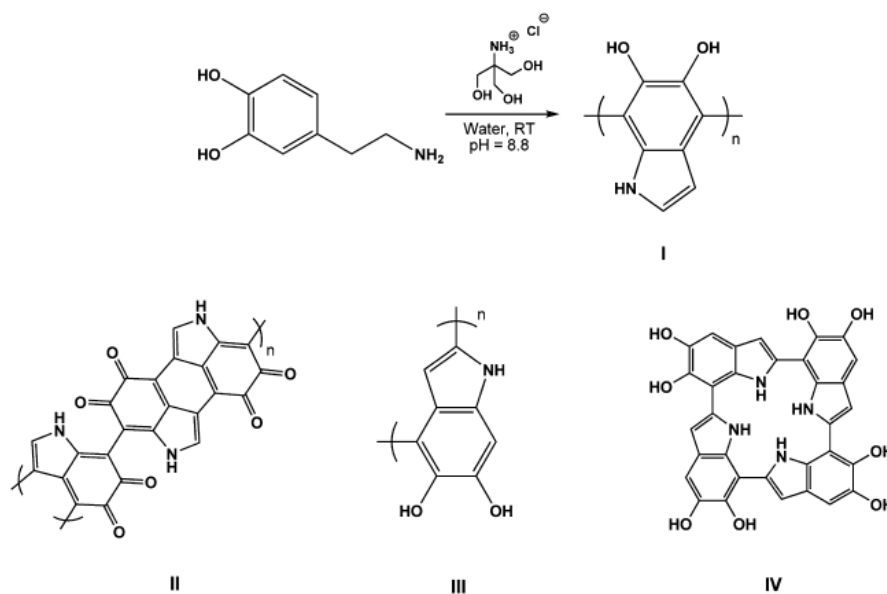


**Figure 3** Proposed PDA structures (Dreyer *et al.*, 2012)

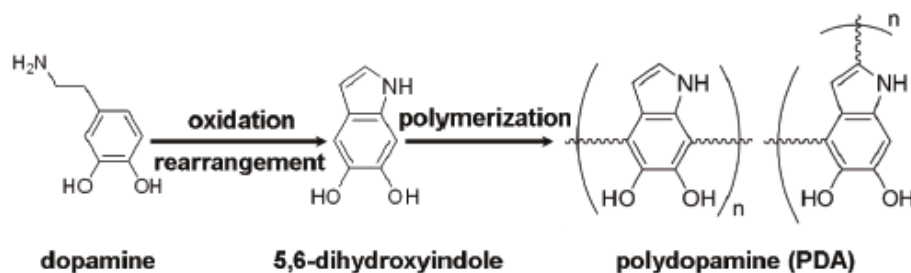


**Figure 4** Oxidative polymerization of dopamine showing two of the possible structures formed (Postma *et al.*, 2009)

### 1.5 Electrochemistry

Electrochemistry investigates properties of ionic conductors and of electric circuits containing ionic conductors, during passage of an electric current through such circuits. Most widely used and studied ionic conductors are aqueous solutions of acids, bases and salts. (Bagotsky, 2006)

In electrochemical reactions, charged particles cross the interface between two states of matter, typically a metallic phase (the electrode) and a conductive solution, or electrolyte. Electrochemical reactions produce a slight unbalance in the electric charges of the electrode and the solution. This is called “potential difference” which can be related to the thermodynamics and kinetics of electrode reactions. Manipulation of the interfacial potential difference is an important way of exerting external control on an electrode reaction.

### 1.5.1 Controlled Potential Coulometry

Controlled potential coulometry is a useful method both as an analytical technique and for the investigation of mechanisms of electrode reactions. In this technique, the potential of the working electrode is held constant, so that oxidation or reduction of the analyte occurs quantitatively (Bard, 1963). The current decreases rapidly and get closes to zero at the end of the reaction. The quantity of electricity is most commonly measured with an electronic integrator or from the reading of a coulometer in series with the cell.

### 1.5.2 Cyclic Voltammetry

Cyclic voltammetry is a very functional electroanalytical technique for the study of electroactive species. Along with the ease of measurement, it is extensively used in many fields of chemistry.

In cyclic voltammetry, potential of a working electrode is cycled and resulting current is measured. The potential of this electrode is controlled versus a reference electrode. Potential is applied as a triangular waveform. This triangular potential sweeps the potential of the electrode between two values (Kissinger & Heineman, 1983).

## 1.6 Raman Spectroscopy

Scattering is a frequently occurring event in nature (Lin-Zhang, 2012). Light can be scattered either in two ways: elastic and inelastic.

Elastic scattering occurs when the energy of incident particles is conserved. This phenomenon is called Rayleigh scattering and it is the reason of the color of blue sky (Young, 1981).

In the Raman Scattering, incident light is inelastically scattered. Energy of incident photons is either gained or lost and this energy is characteristic to the molecule (Kneipp *et al.*, 1999). It was discovered by C.V. Raman, K.S. Krishnan and with the assistance of S. Venkateswaran in 1928 (Raman, 1928).

Polarizability of the molecules induces the Raman Scattering. When the incident photon energy excites vibrational modes of polarizable molecules, scattered photons lose energy and shift in frequency, depending on the amount of the vibrational transition energies.

Raman spectroscopy is a powerful and practical analytical technique which provides information about molecular structures, surface processes, and interface reactions that can be obtained as the outcome of experimental data. It has been increasingly employed in various areas such as chemical, biological analysis and materials science (Vo-Dinh, 1998).

### 1.6.1 Surface Enhanced Raman Spectroscopy

An unusually strong Raman scattering signal was firstly reported in 1974. The signal was observed with pyridine molecules adsorbed on silver electrode surfaces that had been electrochemically roughened by oxidation- reduction cycles (Fleischman *et al.*, 1974).

In 1977, Van Duyne & Jeanmaire and, independently, Albrecht & Creighton suggested that the vastly powerful Raman signal measured from pyridine on a rough silver electrode must be caused by a true enhancement of the Raman scattering efficiency itself. It was concluded that an increase in the number of adsorbed molecules was contributing to the Raman signal. Within a few years, strongly enhanced Raman signals were verified for many different molecules which then named as “SERS-active substrates” (Kneipp *et al.*, 1999). Since then, various kinds of colloidal and solid support based substrates have been widely used for SERS measurements (Li *et al.*, 2004).

Surface-enhanced Raman scattering Spectroscopy attracts great interest because of the possible applications in various fields. Potential use of SERS in detection of neurotransmitters has been commonly studied by the use of colloidal silver solutions. Recently, protonated DA molecule was found to bind bidentately to surface silver atoms through the catechol group which can be evidenced by the comparison between SERS spectra and normal Raman spectra (Lin *et al.*, 2010).

### 1.7 SERS Determination of Dopamine

As it is well known, SERS measurements give clue about the preferred orientation of the adsorbate to the surface of the metal. SERS of dopamine adsorbed on the roughened silver electrode has three strong bands at 1269, 1331 and 1479  $\text{cm}^{-1}$ . These bands are the signature of dopamine molecule. The most intense band at 1479  $\text{cm}^{-1}$  was contributed mainly from stretching of the carbon-carbon bond to which the oxygen's are attached. The band at 1269  $\text{cm}^{-1}$  was assigned to the stretching of the C-O bond of catechol complexed to the silver. Morris *et al.* have concluded that catecholamines are adsorbed on a silver electrode through metal-oxygen bonds and catecholamines form a bidentate complex with silver. On the other hand, when the SERS spectrum of dopamine was examined on silver atoms, the characteristic dopamine spectrum was lost, the intense band at 1476  $\text{cm}^{-1}$  was disappeared and two strong bands at 1287 and 1366  $\text{cm}^{-1}$  were appeared (Lee *et al.*, 1988). According to this spectroscopic evidence, authors have concluded that one of two hydroxyl groups of catechol moiety holds its proton, but the other is deprotonated to attach to the silver surface. In other words, formation of monodentate silver-dopamine complex adsorbed perpendicular to the metal surface was reported.

Therefore, in order to acquire the characteristic dopamine SERS signature, both of the catechol oxygens should take part in the adsorption of dopamine to the silver metal surface, i.e. a bidentate silver-dopamine complex formation is required for the SERS detection of dopamine and other catecholamines. The reactivity of quinone moiety is higher compared to that of dopamine because oxidation of the dopamine molecule produces an electron deficient center that is highly reactive with respect to nucleophiles.

### 1.8 Aim of study

In this study, the objective is to investigate which form of dopamine forms bidentate silver-dopamine complex. Surface interactions between silver and dopamine will be studied by focusing on their oxidation-reduction states. Therefore, dopamine will be oxidized by two methods, electrochemical and by metal ion. In our studies electrochemical oxidation was preferred to eliminate the possible interfering effect of the chemical oxidants on the formed oxidation species and on the SERS measurements. The present study will review the oxidation behavior of dopamine and search an experimental evidence suggesting that reactive dopamine quinone formation may contribute to the adsorption of both of the catechol oxygen's on silver SERS substrate surface. This quinone formation can also be accelerated by metal ions.

Dopamine, containing two hydroxyl groups at the ortho positions to one another, was proved to have the abilities to reduce metal ions to metal nanoparticles, such as Au<sup>+</sup> and Ag<sup>+</sup> (Stokes *et al.*, 1999). Therefore, for further evidence of the reaction between silver nanoparticles and quinone moiety, silver nanoparticles will be prepared via dopamine reduction in which self-polymerization of dopamine produces an adherent polydopamine coating on silver nanoparticle surface.

## CHAPTER 2

### EXPERIMENTAL

#### 2.1 Chemical Reagents

All chemicals and reagents were written in the order of their name, chemical formula, purity and manufacturer name.

- i. **Dopamine hydrochloride**,  $C_8H_{11}NO_2 \cdot HCl$ , Sigma-Aldrich
- ii. **Silver nitrate**,  $AgNO_3$ , Sigma-Aldrich
- iii. **Sodium citrate tribasic dihydrate**,  $Na_3C_6H_5O_7 \cdot 2H_2O$ , Sigma-Aldrich
- iv. **Citric acid monohydrate**,  $C_6H_8O_7 \cdot H_2O$ , Sigma-Aldrich
- v. **Potassium perchlorate**,  $KClO_4$ , Fisher Scientific Company
- vi. **Perchloric acid**,  $HClO_4$ , 60 %, Merck
- vii. **Sodium phosphate dibasic**,  $Na_2HPO_4$ , Fisher Scientific Company
- viii. **Sodium phosphate monobasic**,  $NaH_2PO_4$ , Fisher Scientific Company

All reagents used in this study were in analytical grade. De-ionized water was obtained from Millipore Milli-Q water deionization system. All the glass and plastic materials that were used at experimental procedures were cleaned by soaking in 10%  $HNO_3$  at least for 1 day and then rinsed with distilled water.

#### 2.2 Instrumentation

##### 2.2.1 Field Emission Scanning Electron Microscope (FE-SEM)

FEI Quanta 400F Field Emission Scanning Electron Microscopy located at METU Central Laboratory was used for morphological characterization of Ag nanoparticles. For SEM measurements, the obtained solution was dropped on aluminum stubs and they were dried at room temperature overnight.

##### 2.2.2 Transmission Electron Microscope (TEM)

FEI Biotwin Transmission Electron Microscope located at METU Central Laboratory was used for characterization of DA functionalized Ag nanoparticles.

For TEM measurements, the obtained solution was dropped on carbon-coated copper grids and then they were dried at room temperature overnight.

### **2.2.3 UV-vis Spectrophotometer**

PG Instruments, T80 UV-Visible Spectrophotometer was used to observe optical properties of synthesized silver nanoparticles and oxidation products of DA. Quartz cells were preferred.

### **2.2.4 Raman Spectroscopy**

Renishaw inVia Raman Spectrometer located at METU Central Laboratory was used for Raman measurements of DA, oxidized DA, Ag NPs and Ag electrodes. Laser wavelength was chosen as 632.8 nm throughout the analyses.

### **2.2.5 Electrochemical Measurements**

Gamry PCI4/300 potentiostat was used for electrochemical measurements. Cyclic voltammetry and constant potential coulometry modes were used.

## **2.3 Preparation of Silver Colloid**

Silver colloid was synthesized by chemical reduction method (Lee & Meisel, 1982). According to this,  $10^{-3}$  M  $\text{AgNO}_3$  was prepared by dissolving 90 mg of it, in 500 ml of de-ionized  $\text{H}_2\text{O}$ . The solution was heated and stirred until boiling. 10 ml of 1% (w/v) of  $\text{Na}_3\text{C}_6\text{H}_5\text{O}_7$  solution was added to boiling solution. The solution was kept boiling for 1 hour. Resulting colloid has a pale, greenish-yellow color. Uv-vis and SEM characterizations were applied. Particles synthesized with this method give absorption maximum at 420 nm with UV-vis spectrometer (Lee & Meisel, 1982). According to SEM image, particle size is 70 nm averagely (Figure 5).

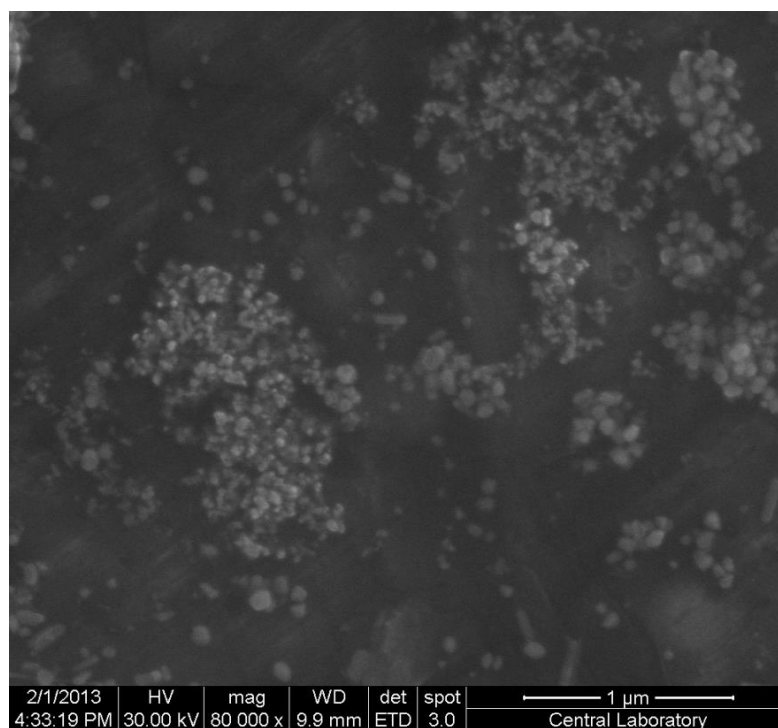


**Figure 5** SEM image of synthesized Ag colloid

#### **2.4 Preparation of Surface Modified Silver Nanoparticles with Dopamine**

DA coated silver nanoparticles were prepared based on a previous study (Ma *et al.*, 2011). Different concentrations and amounts of AgNO<sub>3</sub>, NaOH and DA were mixed respectively. Incubation time was 1 hour. Plenty of experiments were conducted to determine the optimum combination of reagents. Synthesized nanoparticles were verified with UV-vis spectrometer and characterized by SEM and TEM.

#### **2.5 Electrochemical Oxidation of Dopamine**

Electrochemical oxidation of DA was worked by using platinum and silver electrode as working electrodes. Silver wire was chosen as reference electrode. Pt electrode was the counter electrode for both studies. Effect of different conditions on oxidation process - in terms of pH, medium and applied potential - were investigated. Resultant products were identified by UV-vis spectrometer.

DA solution was freshly prepared for each experiment. Concentration of solution was kept constant at 10<sup>-3</sup> M. 2.3 mg of DA was dissolved in 15 ml of relevant buffer for each trial. Before starting, UV-vis analysis was applied to DA solution to make sure its validity. Normally, DA gives two absorption maxima at 230 and 280 nm.

Throughout all electrochemical studies; controlled potential coulometry programme was used to oxidize DA.

This mode of Gamry Instrument applies the adjusted potential constantly, during the programmed time. 10 minutes were chosen to apply the relevant potential as each period of oxidation. At the end of each period, the product was followed with UV-vis spectrometry.

### 2.5.1 Oxidation of Dopamine by Platinum Electrode

Various conditions were tried to oxidize DA by using Pt electrode as working electrode.

#### 2.5.1.2 Oxidation of Dopamine in Neutral Medium

0.1 M phosphate buffer was prepared with sodium phosphate dibasic and sodium phosphate monobasic at pH 6. DA solution was prepared in this buffer. 0.6 V was applied. Cyclic voltammogram of Pt electrode in pH 6 PBS, without and with DA are demonstrated in Figure 6 and Figure 7, respectively.

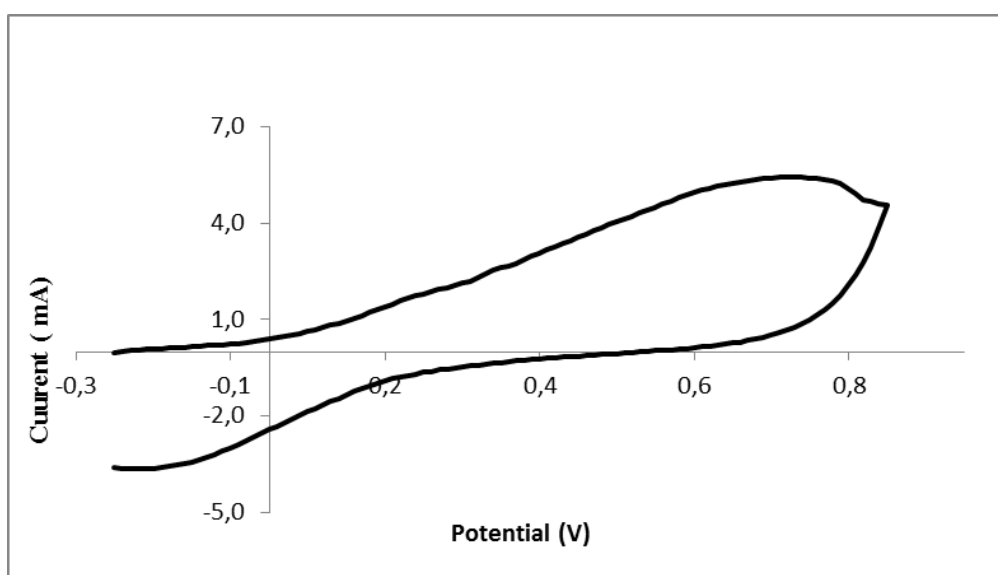


**Figure 6** Cyclic voltammogram of pH 6 PBS, at Pt electrode (from -0.2 V to 0.8 V)



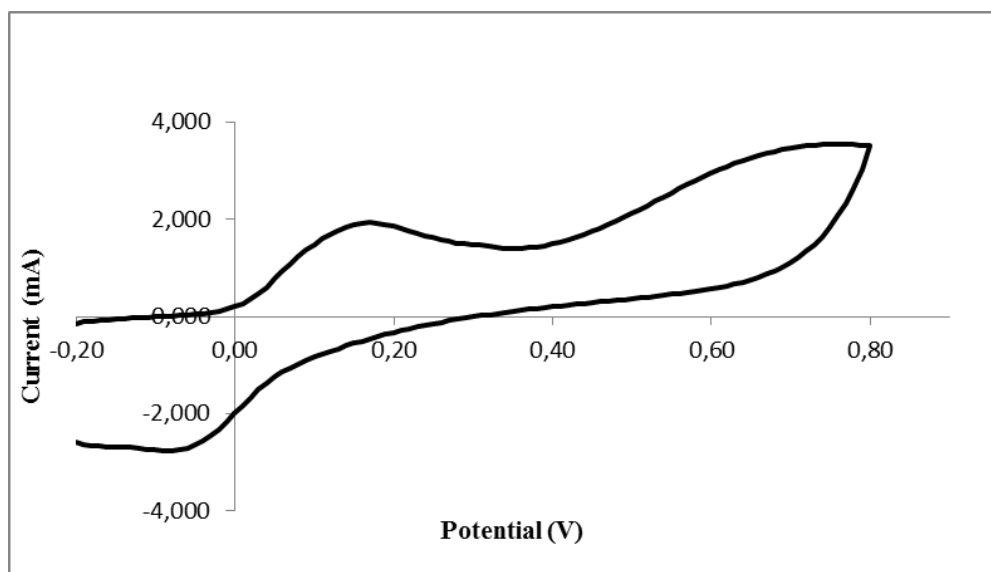


**Figure 7** Cyclic voltammogram of DA, in pH 6 PBS, at Pt electrode (from -0.2 V to 0.8 V)

### 2.5.1.3 Oxidation of Dopamine in Acidic Medium

0.1 M citrate buffer was prepared with citric acid and sodium citrate so as to be at pH 3. DA solution was prepared in this buffer. 0.6 V was applied.

Cyclic voltammogram of Pt electrode in pH 3 citrate buffer, without and with DA are demonstrated in Figure 8 and Figure 9, respectively.

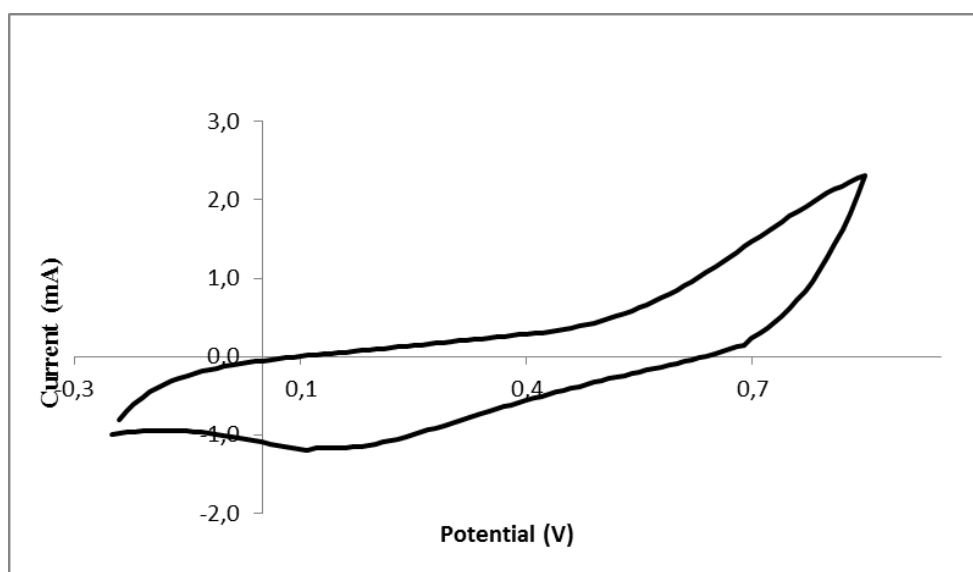


**Figure 8** Cyclic voltammogram of pH 3 citrate buffer, at Pt electrode (from -0.2 V to 0.8 V)

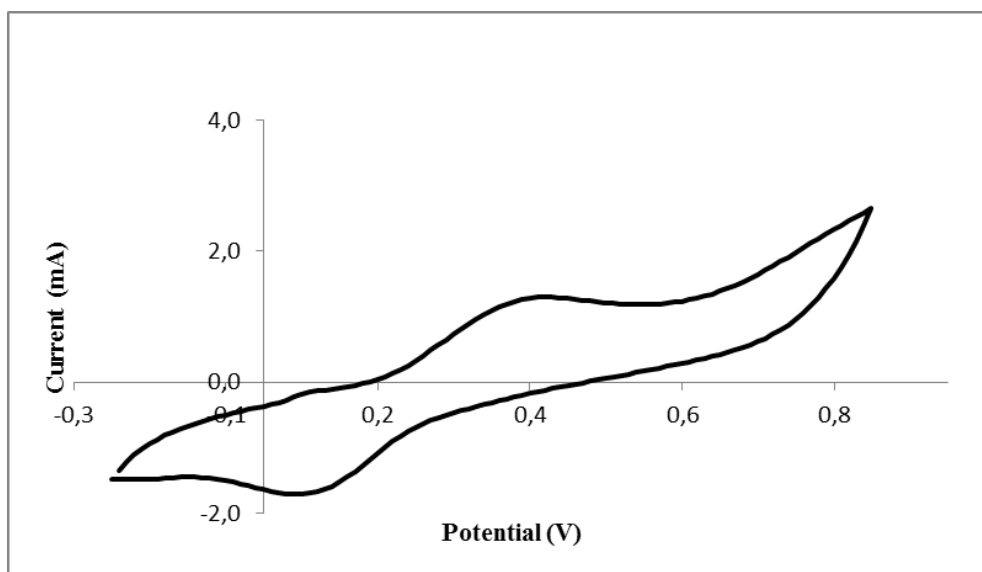


**Figure 9** Cyclic voltammogram of DA, in pH 3 citrate buffer, at Pt electrode (from -0.2 V to 0.8 V)

## 2.5.2 Oxidation of Dopamine by Silver Electrode

Various conditions were tried to oxidize DA on silver electrode. 0.1 M  $\text{KClO}_4$  solution was prepared as the electrolyte. pH of the prepared  $\text{KClO}_4$  solution was measured as 7.

### 2.5.2.1 Oxidation of Dopamine in Neutral Medium

DA solution was prepared in  $\text{KClO}_4$ . 0.6 V was applied but since it decomposed DA immediately, 0.2 V was decided to be applied for this part. Cyclic voltammogram of Ag electrode in pH 7  $\text{KClO}_4$  without and with DA are demonstrated in Figure 10 and Figure 11, respectively.

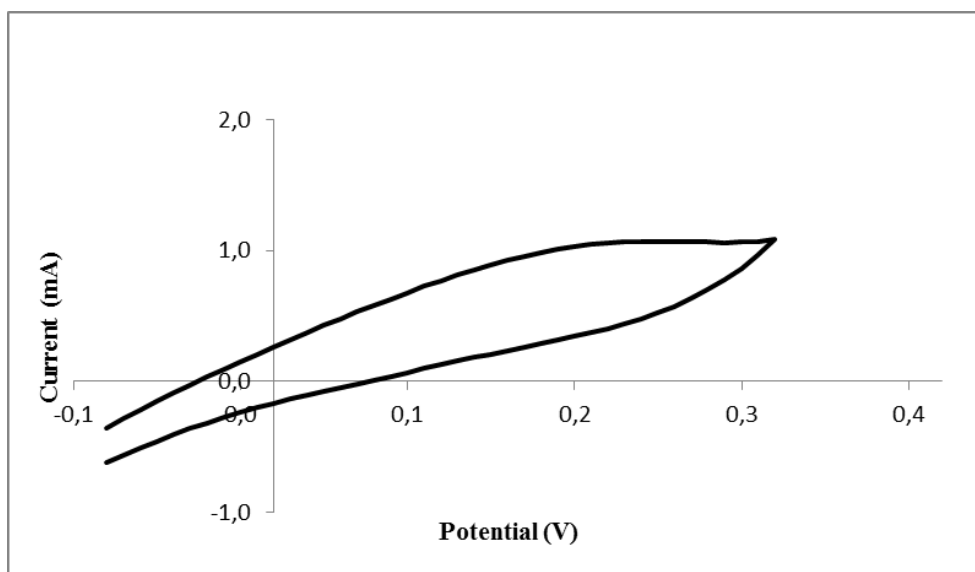


**Figure 10** Cyclic voltammogram of pH 7  $\text{KClO}_4$ , at Ag electrode (from -0.1 V to 0.3 V)

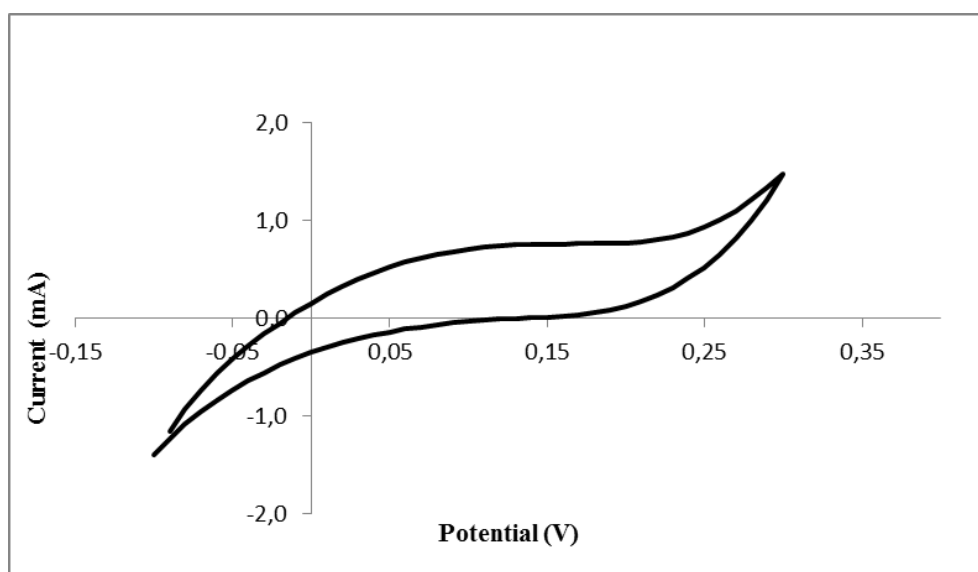


**Figure 11** Cyclic voltammogram of DA, in pH 7  $\text{KClO}_4$ , at Ag electrode (from -0.1 V to 0.3 V)

### 2.5.2.2 Oxidation of Dopamine Acidic Medium

pH of  $\text{KClO}_4$  solution was adjusted to 3 with  $\text{HClO}_4$ . DA solution was prepared in this solution. 0.35 V, 0.30 V, 0.25 V and 0.20 V were scanned to determine the optimum oxidative condition. Cyclic voltammogram of Ag electrode in pH 3  $\text{KClO}_4$  without and with DA are demonstrated in Figure 12 and Figure 13, respectively.

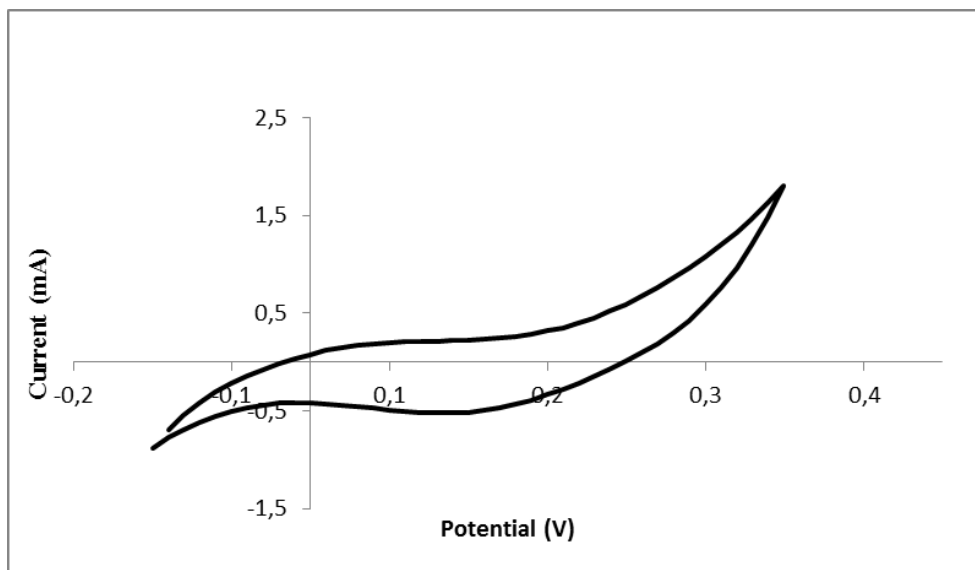


**Figure 12** Cyclic voltammogram of pH 3 KClO<sub>4</sub>, at Ag electrode (from -0.1 V to 0.3 V)

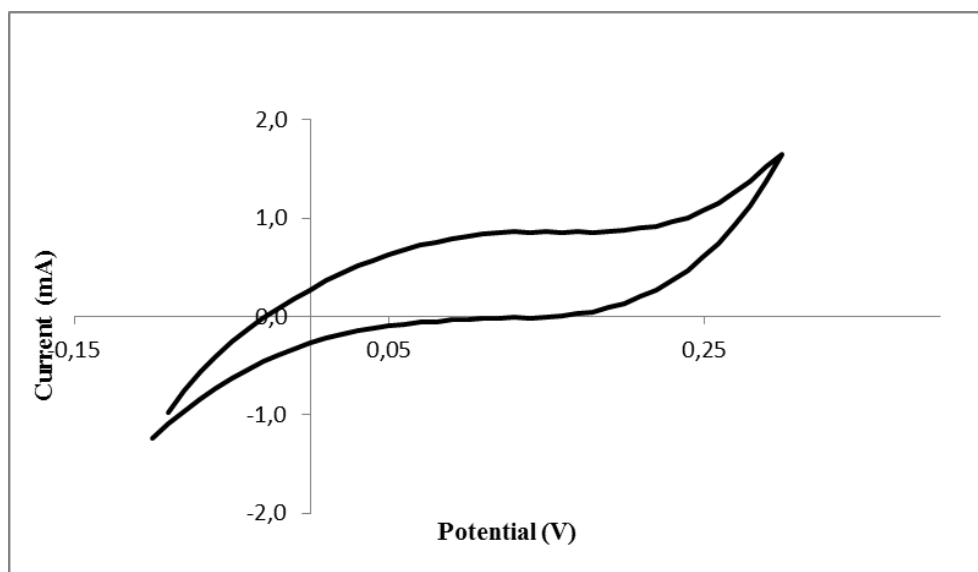


**Figure 13** Cyclic voltammogram of DA, in pH 3 KClO<sub>4</sub>, at Ag electrode (from -0.1 V to 0.3 V)

## 2.6 Raman Spectroscopic Analysis

In order to apply Raman Spectroscopy, electrochemically oxidized products and DA itself were mixed with silver colloid, dropped on glass surface and left to dry before analysis. Synthesized Ag NPs also dropped and dried on glass surface.

Silver electrode was roughened in accordance with previously studied procedure (Lee *et al.*, 1988). Cyclic voltammetry and controlled potential coulometry was applied 3 times in turns to provide porosity. Electrode was cycled from -0.3 V to 0.3 V at 10 mV/s scan rate in 0.1 M KCl. 3 cycles were applied. After that, controlled potential coulometry was done applied by pausing at -0.3 V for 8 seconds, then at 0.3 V for 3 seconds. Roughened electrode surfaces were analyzed directly.

## CHAPTER 3

### RESULTS AND DISCUSSION

This thesis consists of two parts. In the first part of the study, electrochemical oxidation of dopamine was studied by using platinum and silver electrodes as working electrode. Electrolysis experiments were conducted at different pH and applied potential conditions. The formed oxidation products of dopamine were identified by utilizing UV-vis spectrometry. SERS measurements of the electrode surface used in the oxidation studies and the oxidation products formed were done in order to shed a light to the adsorption mechanism of dopamine to the silver metal surface. In other words, to understand in which oxidation form of dopamine, both of the catechol oxygens take a part in the adsorption.

In the second part, dopamine was oxidized by silver metal ions. While dopamine was oxidized, silver nitrate was reduced, constituting silver nanoparticles. The conditions required for the synthesis of the nanoparticles were optimized. Morphological and optical characterizations of these dopamine functionalized nanoparticles were performed by SEM, TEM and UV-vis spectrometry. SERS spectrum of the dopamine coating of these silver nanoparticles was measured again for investigating the nature of dopamine silver nanoparticle interaction.

#### 3.1 Electrochemical Oxidation of Dopamine on Platinum Electrode

As a start, Pt electrode was chosen as both working and counter electrodes. Silver wire was used as reference electrode. Controlled potential coulometry was applied to dopamine. It exerted the preferred potential constantly, during ten minutes' of periods. Electrolysis experiments were tried in both neutral and acidic media which then exhibited different oxidation products. Oxidized products were identified with UV-vis spectrometry at the end of each ten minutes to follow the reaction.

##### 3.1.1 Oxidation of Dopamine in Neutral Medium

DA was prepared in pH 6 phosphate buffer based on a previous study (Sun *et al.*, 2007). PBS was used as the electrolyte in order to provide the passage of electric current. According to CV experiment, oxidation peak was appeared at 0.6 V, as demonstrated in some other studies (Wightman & Venton, 2003). Controlled potential coulometry was applied for 10 minutes. At the end of the electrolysis, there wasn't any deposition on the surface of electrodes and the color of solution turned into bright orange which indicates the formation of dopamine-chrome (Bisaglia *et al.*, 2007). The UV-vis spectrum of this oxidation product shows a new absorption maximum at 480 nm (Figure 14) which also proves the formation of dopamine-chrome form (Wei *et al.*, 2010) (Kerry & Rice-Evans, 1999).

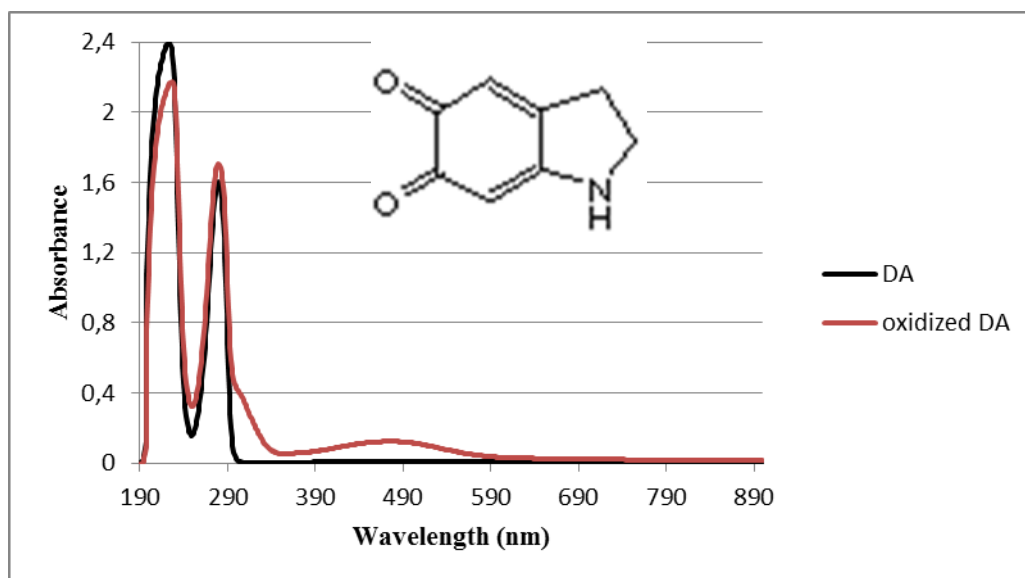


**Figure 14** UV-vis spectrum of oxidation product on Pt electrode, in pH 6 PBS, at 0.6 V

At neutral and basic pH values, dopamine is oxidized to dopamine-quinone which then rapidly cyclizes into leucoaminochrome intermediate because of highly nucleophilic side chain  $\text{NH}_2$  group's attack. This intracyclization is followed by the oxidation of leucoaminochrome to dopamine-chrome (Tse *et al.*, 1976) (Borovansky *et al.*, 2006). Figure 15 demonstrates this case.

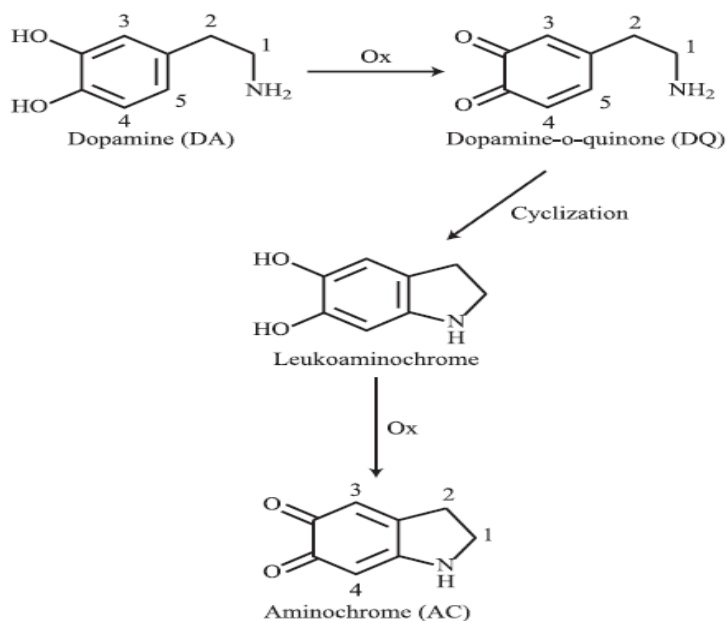


**Figure 15** Aminochrome(dopaminechrome) formation mechanism (Bisaglia *et al.*, 2007)

### 3.1.2 Oxidation of Dopamine in Acidic Medium

DA solution in pH 3 citrate buffer was tried to be oxidized. 0.6 V was applied for 10 minutes as each oxidation cycle. After first cycle of electrolysis, the color of solution changed into light yellow which indicates the formation of dopamine-quinone (Bisaglia *et al.*, 2007). UV-vis spectrum of this oxidation product proved its formation with the appearance of absorption maximum at 380 nm (Figure 16) Peaks can be seen more clearly from Figure 17.

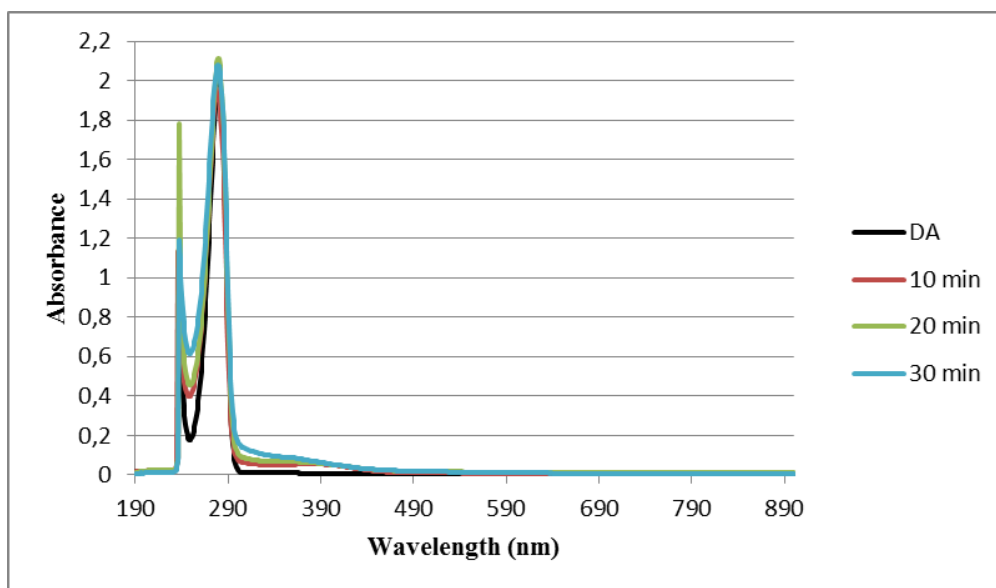


Figure 16 UV-vis spectra of DA oxidation products on Pt electrode, in pH 3 citrate buffer, at 0.6 V

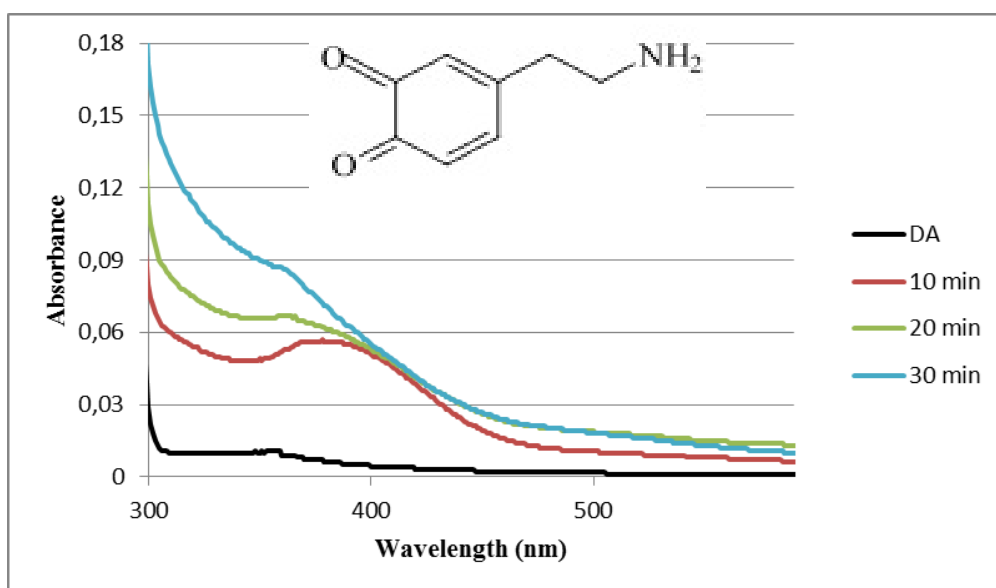


Figure 17 UV-vis spectra of DA oxidation products on Pt electrode, in pH 3 citrate buffer, at 0.6 V



At low pH values, side chain  $\text{NH}_2$  group of dopamine is protonated. This inhibits the nucleophilic attack of amine group which causes the intracyclization that leads to dopamine-chrome formation. In fact, it happens but too slow to occur during electrolysis. (Tse *et al.*, 1976).

### 3.2 Electrochemical Oxidation of Dopamine on Silver Electrode

After identification of oxidation products by working with Pt electrode, dopamine was electrolyzed with silver electrode in accordance with the purpose of study. Pt electrode was chosen as counter electrode, silver wire was used as reference electrode. This time DA was prepared in  $\text{KClO}_4$ . PBS was given up as the electrolyte to avoid undesired complication of medium because of ions it contains. Likewise, citrate buffer was not chosen since it has reducing effect on silver.

Before electrolysis, silver electrode surface was roughened.

#### 3.2.1 Oxidation of Dopamine in Neutral Medium

DA was prepared in  $\text{KClO}_4$  having a pH value of 7. Firstly, 0.6 V was chosen to apply since it worked in Pt electrode studies. DA solution decomposed as soon as the voltage was applied. It changed into heterogeneous dark-brown slurry with particles in it. This outcome was polydopamine as stated in other studies (Wei *et al.*, 2010) (Postma *et al.*, 2009). Moreover, according to studies (Miyazaki & Asanuma, 2009) (Bisaglia *et al.*, 2007), oxidation of DA yields DA-quinone followed by cyclization of the quinone to give leukoaminochrome and its subsequent oxidation to DA-chrome. Then, it rearranges to 5,6-dihydroxyindole, which can be oxidized to indole-5,6-quinone and finally polymerize to form melanin. Polymerization mechanism is depicted in Figure 18.

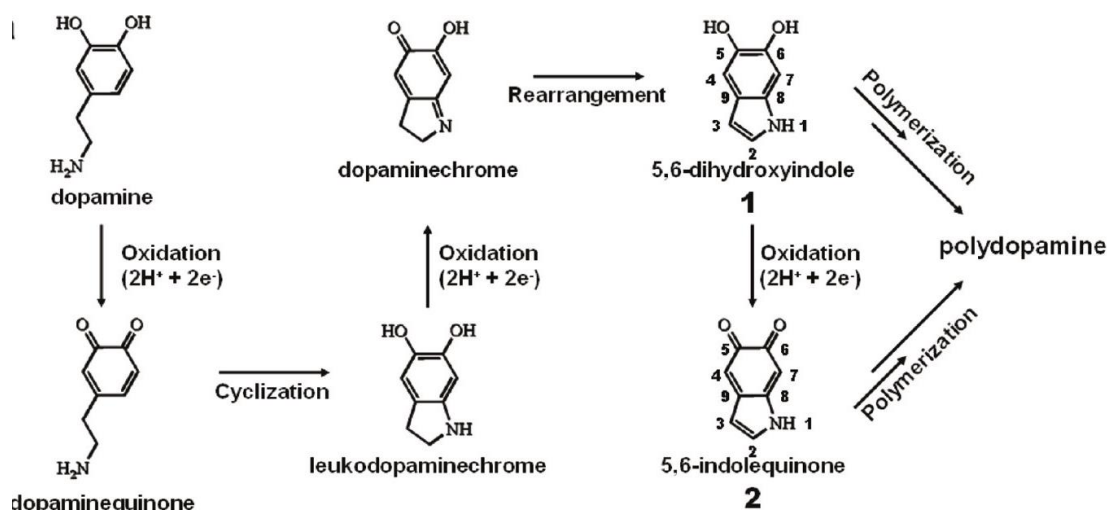
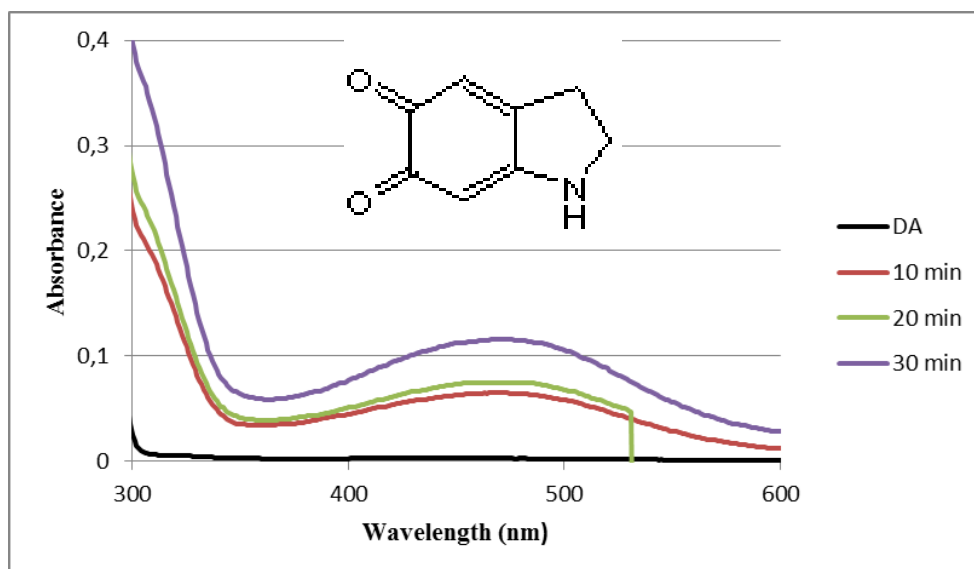


Figure 18 Polymerization of dopamine (Jiang *et al.*, 2011)

After that, applied voltage was decreased. 0.2 V was strong enough to oxidize dopamine without polymerization. It was applied constantly during ten minutes' of periods. Starting with the first ten minutes, orange color of dopamine-chrome was observed. This formation was also demonstrated with

the appearance of absorption maximum at 475 nm in the UV-vis spectra of the products (Figure 20). Figure 19 demonstrates the dopamine-chrome peaks apparently.



**Figure 19** UV-vis spectra of DA oxidation products on Ag electrode, in pH 7 KClO<sub>4</sub>, at 0.2 V

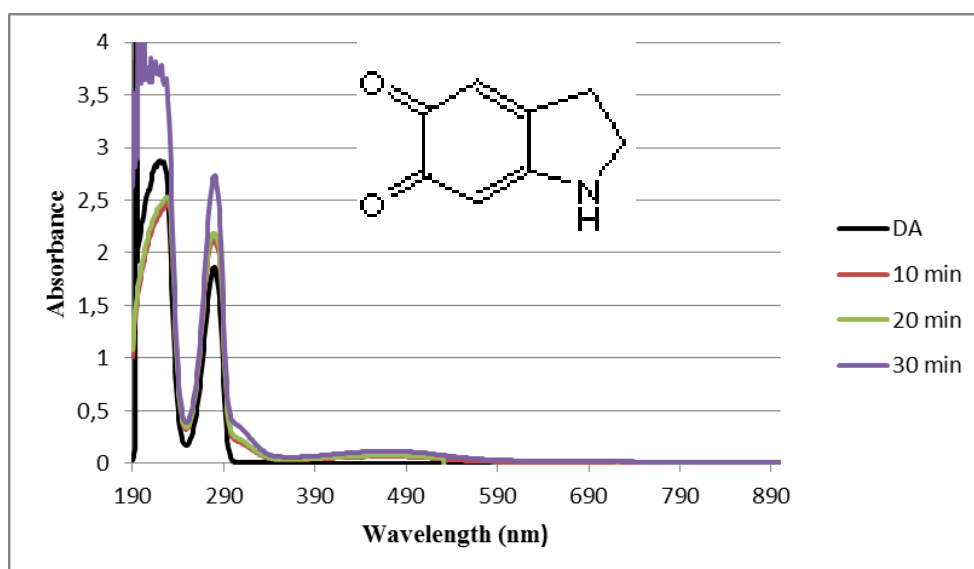


**Figure 20** UV-vis spectra of DA oxidation products on Ag electrode, in pH 7 KClO<sub>4</sub>, at 0.2 V

### 3.2.2 Oxidation of Dopamine in Acidic Medium

DA was prepared in KClO<sub>4</sub> and pH of the solution was adjusted to 3. As a start, 0.35 V potential was tried, but at this potential all DA was polymerized.

Then, 0.3 V and 0.25 V were experienced. Color changes without polymer formation in the electrolysis medium were obtained at 0.25 V. The UV-VIS spectra of the reaction products are given in Figure 21. During first 30 minutes of electrolysis, dopamine-quinone formation was observed according to UV-vis spectra. Absorption maxima were appeared at about 390 nm (Figure 22). At longer reaction times, on the other hand, the absorption maximum shifted towards red 430nm (Figure 23) and dopamine-chrome formation was started to appear in the solution with its typical orange color.

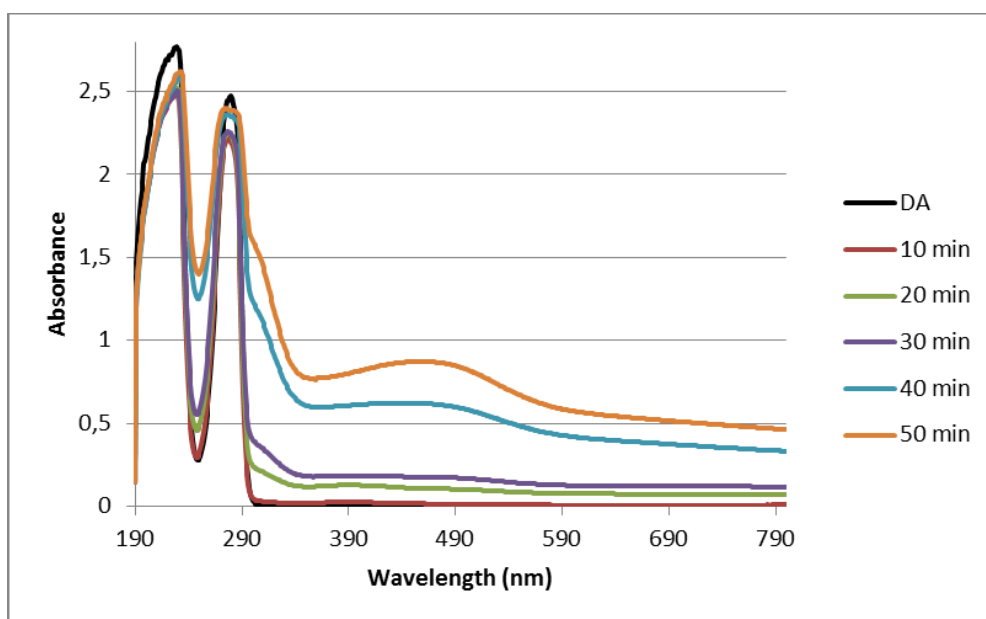


**Figure 21** UV-vis spectra of DA oxidation products on Ag electrode, in pH 3  $\text{KClO}_4$ , at 0.25 V

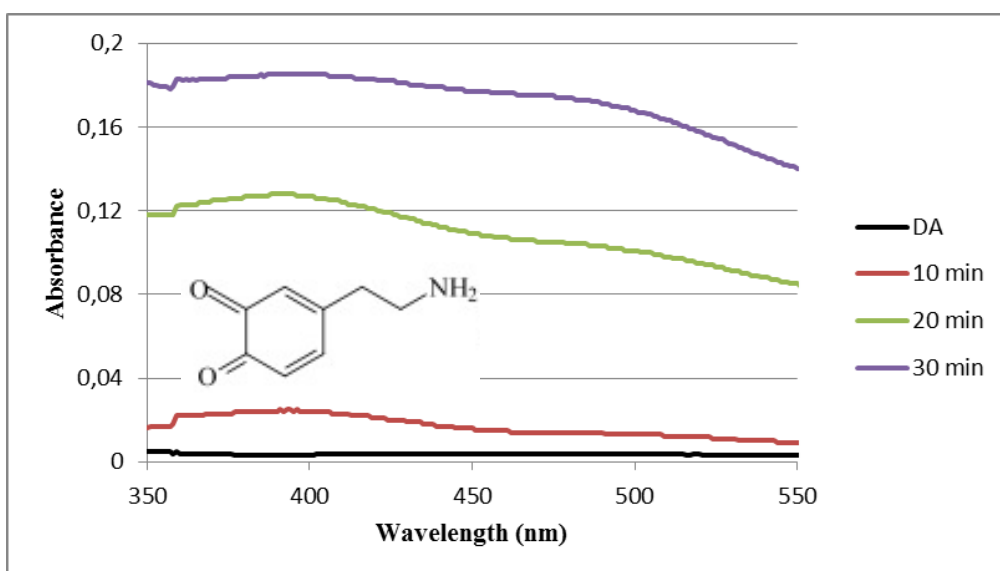


**Figure 22** UV-vis spectra of DA oxidation products on Ag electrode, in pH 3  $\text{KClO}_4$ , at 0.25 V

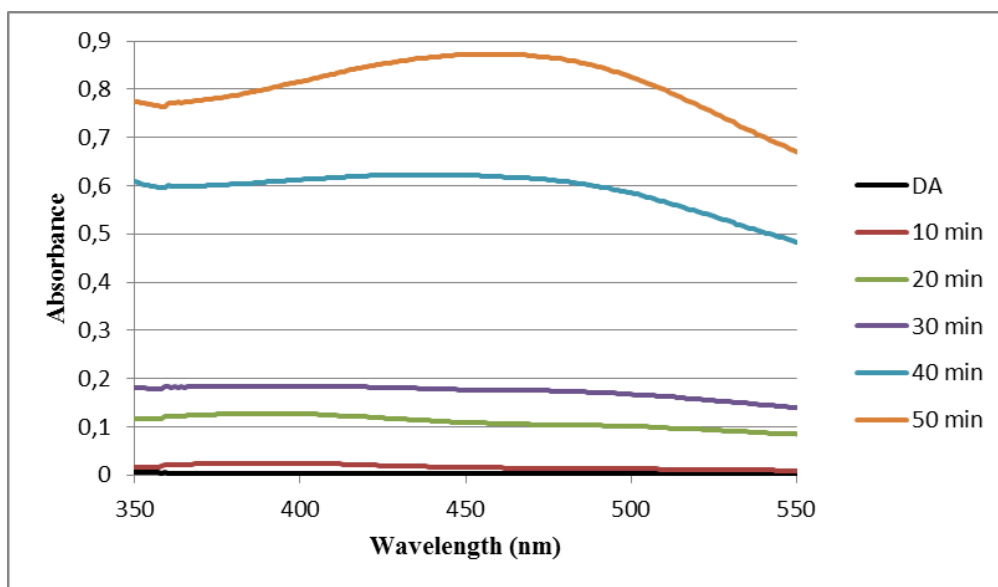


**Figure 23** UV-vis spectra of DA oxidation products on Ag electrode, in pH 3 KClO<sub>4</sub>, at 0.25 V

Furthermore, 0.2 V was applied. But this voltage didn't have any oxidizing effect on dopamine solution as can be seen from Figure 24.

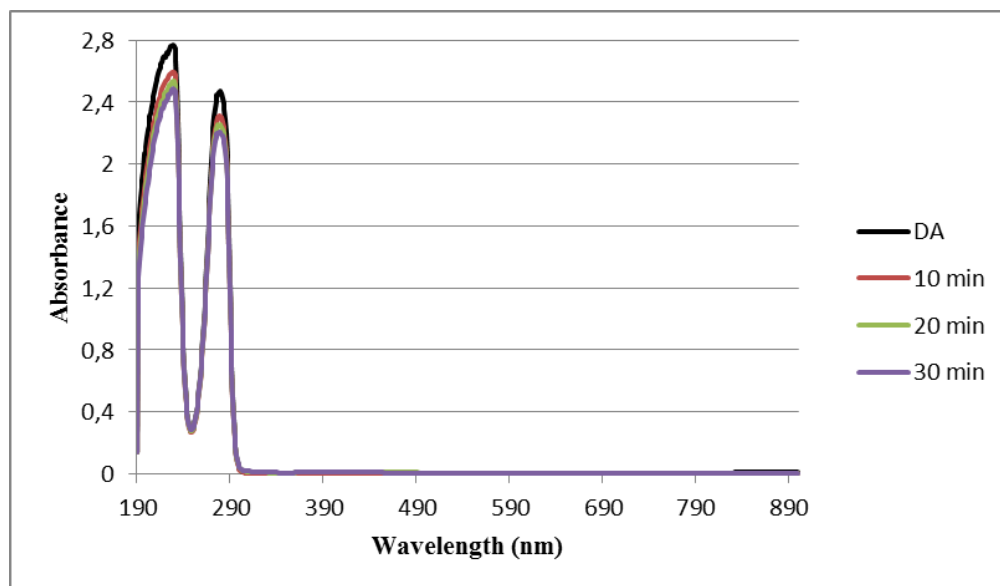


**Figure 24** UV-vis spectra of DA oxidation products on Ag electrode, in pH 3 KClO<sub>4</sub>, at 0.20 V

### 3.3 Preparation of Dopamine Functionalized Silver Nanoparticles

According to Ma *et al.*, dopamine can reduce  $\text{Ag}^+$  to form monodispersed AgNPs and functionalize the produced AgNPs. At the same time, dopamine itself is oxidized. Various experiments were carried out to have a better understanding about formation of dopamine functionalized silver nanoparticles and to optimize the conditions. This claim was verified through a series of experiments in which various DA,  $\text{AgNO}_3$  and NaOH concentrations were used. These experimental conditions can be separated into two groups in terms of the concentration levels of the precursors. In one group concentrations were in the micromolar range whereas in the other group millimolar concentration range was applied.

#### 3.3.1 Preparation of DA functionalized Ag NPs at $\mu\text{M}$ concentration level of precursors

The summary of the experimental conditions in terms of the concentrations of the precursors and the base at micromolar level are presented in Table 1. (Given values are the final concentrations of each component.) The morphology and the change in the plasmon absorption behaviors of the synthesized particles were investigated through TEM and UV-vis absorption Spectrometry respectively.

**Table 1** The summary of the experimental conditions in terms of the concentrations of the precursors (at micromolar level) and the base

Exp.	Conc. Of $\text{AgNO}_3$	Conc. Of DA	Conc. Of NaOH
1	80 $\mu\text{M}$	10 $\mu\text{M}$	250 $\mu\text{M}$
2	80 $\mu\text{M}$	10 $\mu\text{M}$	750 $\mu\text{M}$
3	80 $\mu\text{M}$	10 $\mu\text{M}$	1 mM
4	80 $\mu\text{M}$	20 $\mu\text{M}$	250 $\mu\text{M}$
5	80 $\mu\text{M}$	20 $\mu\text{M}$	750 $\mu\text{M}$
6	80 $\mu\text{M}$	20 $\mu\text{M}$	1 mM
7	80 $\mu\text{M}$	40 $\mu\text{M}$	250 $\mu\text{M}$
8	80 $\mu\text{M}$	40 $\mu\text{M}$	750 $\mu\text{M}$
9	80 $\mu\text{M}$	40 $\mu\text{M}$	1 mM

The observations can be stated as follows. When final concentrations of  $\text{AgNO}_3$  and DA were at  $\mu\text{M}$  levels, small sized DA functionalized Ag NPs were synthesized. The prepared dispersions were very stable and their colors were bright yellow (Figure 25).

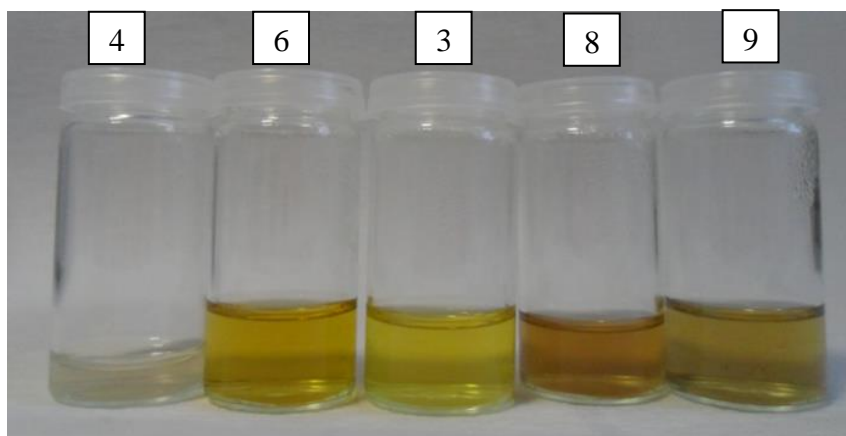


**Figure 25** The appearance of the DA functionalized Ag NPs synthesized at  $\mu\text{M}$  concentration levels of the precursors, as stated in Table 1

The pH of the medium is very important both for oxidation and polymerization regarding the formation of catecholate anion.  $250 \mu\text{M}$  NaOH concentration was not sufficient for the formation of the nanoparticles, instead DC was formed in the solution. There are two acidic protons in DA having  $\text{pK}_1$  and  $\text{pK}_2$  values of 8.87 and 10.63 corresponding to the catechol hydroxyl and ethyl ammonium groups of DA, respectively (McGlashen *et al.*, 1990). Therefore, the solution should have a basic pH value. In the synthesis of the dopamine functionalized silver nanoparticles, optimum condition of NaOH was found as 1 mM, which refers to pH 10.5 in the final solution, suitable for the catecholate formation. TEM image of particles are shown in Figure 26 and Figure 27. Accordingly, smaller sized NPs were obtained at  $80 \mu\text{M}$   $\text{AgNO}_3$  and  $10 \mu\text{M}$  DA, where  $\text{AgNO}_3$  to DA ratio was 8, was used. Size distribution is in between 5 nm and 45 nm. When the ratio was 2, larger particles formed as can be seen in Figure 27. Their sizes were ranged from 35 to 55 nm. Results show that larger  $\text{AgNO}_3$  to DA ratio generated smaller particles.

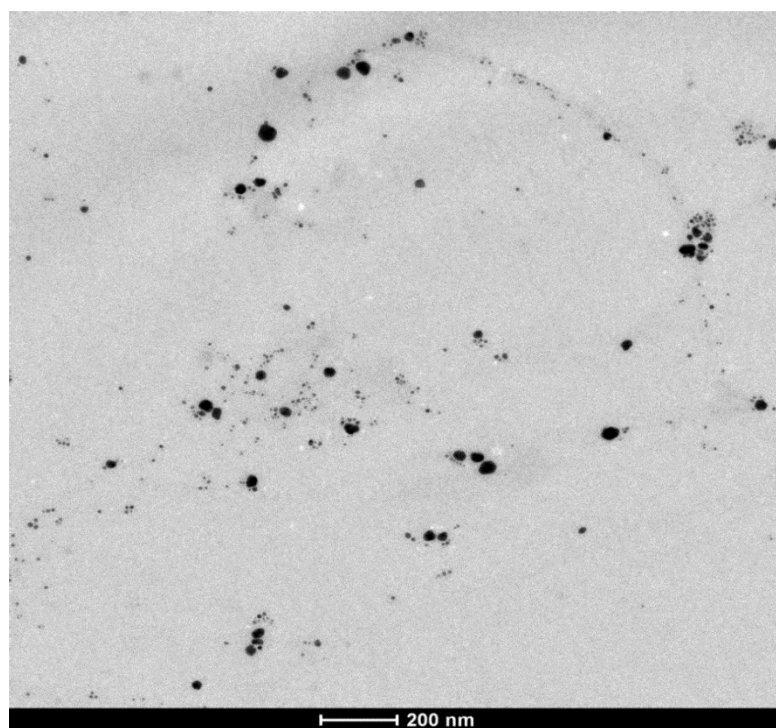


**Figure 26** TEM image of Ag NPs formed in experiment 3 in Table 1 (80  $\mu\text{M}$   $\text{AgNO}_3$ , 10  $\mu\text{M}$  DA & 1 mM NaOH)

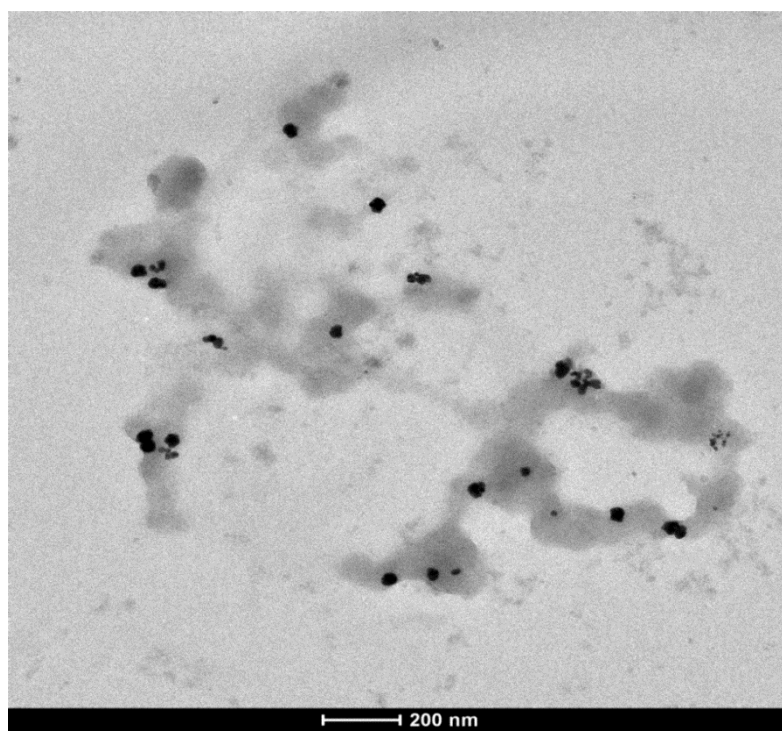


**Figure 27** TEM image of Ag NPs formed in experiment 9 in Table 1 (80  $\mu\text{M}$   $\text{AgNO}_3$ , 40  $\mu\text{M}$  DA & 1 mM NaOH)

UV- vis spectra of NPs (Figure 28) are also supporting these observations. A red shift is observed in the plasmon absorption of the silver nanoparticles as the size of the particles increase. As one can see, dispersion of the particles synthesized with excessive  $\text{AgNO}_3$  has the absorption maximum located at 417 nm while particles prepared at  $\text{AgNO}_3$  to DA ratio of 2 has the absorption maximum at 440 nm. Another observation was related with the duration of the particle synthesis. The incubation time was 1 hour for the synthesis of the silver nanoparticles when  $\text{AgNO}_3$  to DA ratio was 4 and 8 whereas it was 24 hours when the ratio was 2. This fact indicates that amount of  $\text{AgNO}_3$  seems to affect the reaction kinetics; excess oxidant speeds up the reaction.

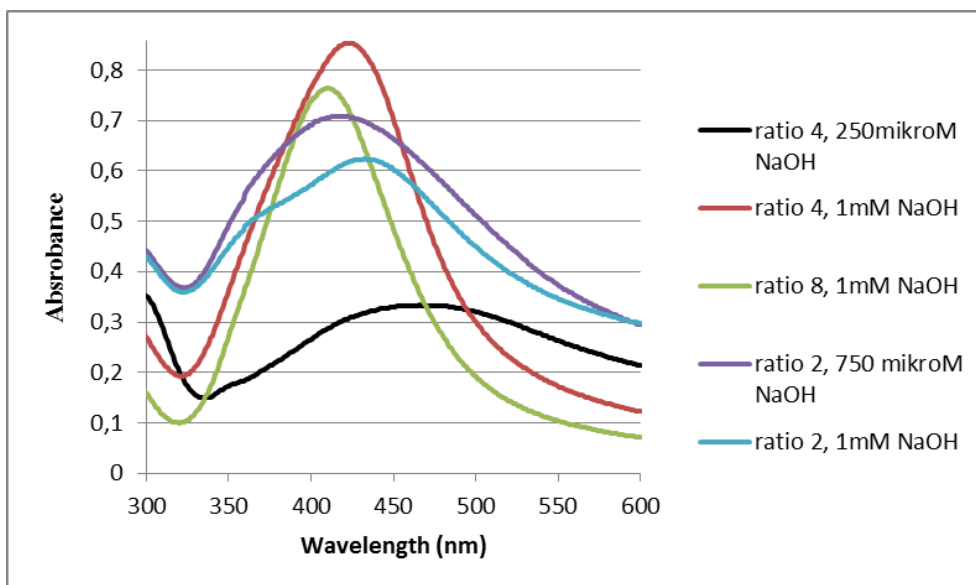


**Figure 28** UV-vis spectra of Ag NPs synthesized with different amounts of  $\text{AgNO}_3$ , DA and NaOH

### 3.3.2 Preparation of DA functionalized Ag NPs at mM concentration level of precursors

Further investigation was continued with the higher concentrations of  $\text{AgNO}_3$  and DA. When mM concentrations of  $\text{AgNO}_3$  and DA were employed, the same concentrations of NaOH used in previous experiments (Table 2) exhibited a polymerization effect (Figure 29). 250  $\mu\text{M}$ , 750  $\mu\text{M}$  and 1 mM NaOH were tried but nanoparticles couldn't form, instead all DA directly polymerized. Adding concentrated NaOH stimulates the process starting with the intracyclization and reaction continues until polydopamine forms.

**Table 2** The summary of the experimental conditions in terms of the concentrations of the precursors (at millimolar level) and the base

Exp.	Conc. Of $\text{AgNO}_3$	Conc. Of DA	Conc. Of NaOH
10	8 mM	1 mM	250 $\mu\text{M}$
11	8 mM	1 mM	1 mM
12	8 mM	2 mM	750 $\mu\text{M}$
13	8 mM	2 mM	1 mM



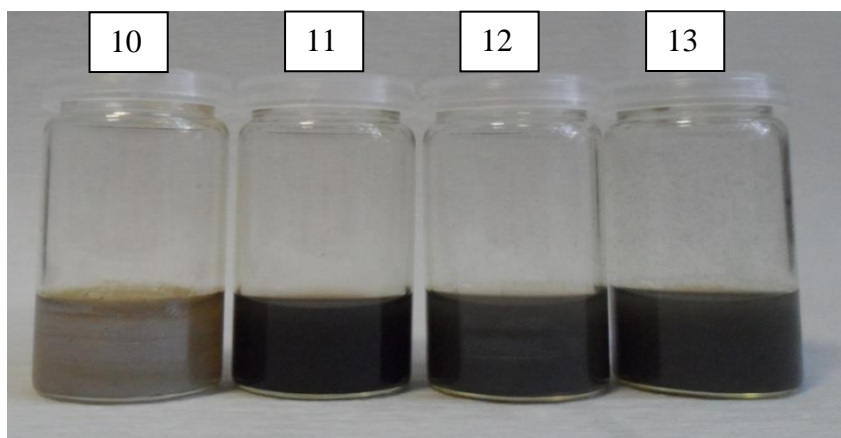


**Figure 29** Polymerized DA

Since we couldn't obtain NPs at highly basic medium, decreasing NaOH concentration was seemed to be a solution (Table 3).

**Table 3** The summary of the experimental conditions in terms of the concentrations of the precursors (at millimolar level) and the base (low concentrations of NaOH)

Exp.	Conc. Of AgNO <sub>3</sub>	Conc. Of DA	Conc. Of NaOH
14	8 mM	1 mM	25 μM
15	8 mM	1 mM	10 μM
16	8 mM	2 mM	25 μM
17	8 mM	2 mM	10 μM

Experiments 14 and 16 (with 25 μM NaOH) formed nanoparticles but they were noticeably larger. They looked like Ag colloid synthesized with method stated by Lee *et al.* (Figure 30).

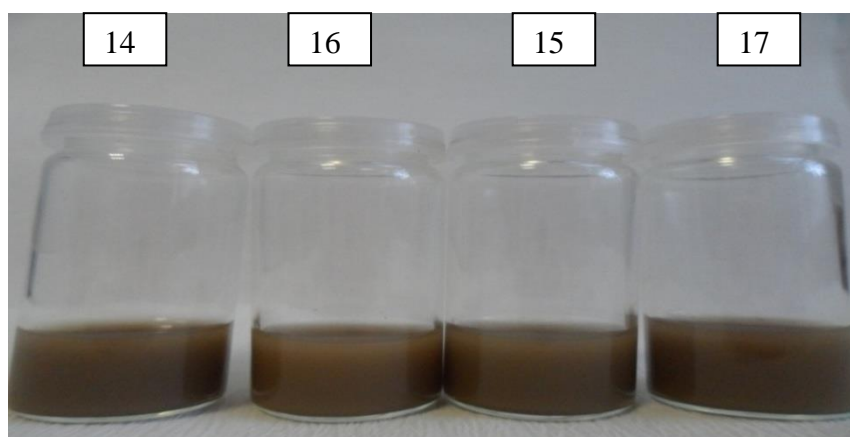


**Figure 30** DA functionalized Ag NPs dispersions synthesized at mM concentration levels of the precursors, as stated in Table 3

Figure 31 and Figure 32 demonstrate SEM images of particles formed at 25  $\mu\text{M}$  of NaOH. Homogenous and dispersed nanoparticles were observed. At 8mM  $\text{AgNO}_3$  and 1 mM DA, ratio was 8; particle size was about 50 nm averagely (Figure 31). However, it was around 75 nm (Figure 32) when the ratio was 4. Likewise in  $\mu\text{M}$  level studies, adding more oxidizing agent provides smaller – sized particles. As discussed before the size of nanoparticle is highly dependent on parameters influencing the rate constant for the spontaneous oxidation of dopamine. The detailed kinetic model for the oxidation of dopamine suggests that the abstraction of a hydrogen atom by an oxidant from the catecholate anion of the dopamine is the rate-determining step (Herlinger *et al.*, 1995). The subsequent ring closing reaction of semiquinone to dopaminochrome is relatively fast. Therefore, the rate constant for the spontaneous oxidation of dopamine is mostly influenced by pH and the concentrations of  $\text{AgNO}_3$  and dopamine.

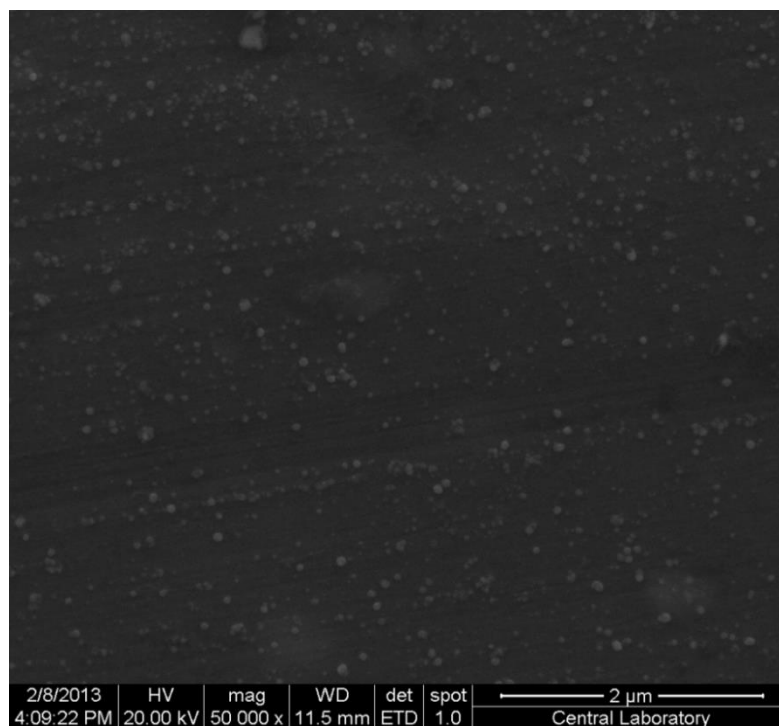


**Figure 31** SEM image of Ag NPs, experiment 14 in Table 3 (8mM  $\text{AgNO}_3$ , 1 mM DA & 25  $\mu\text{M}$  NaOH)

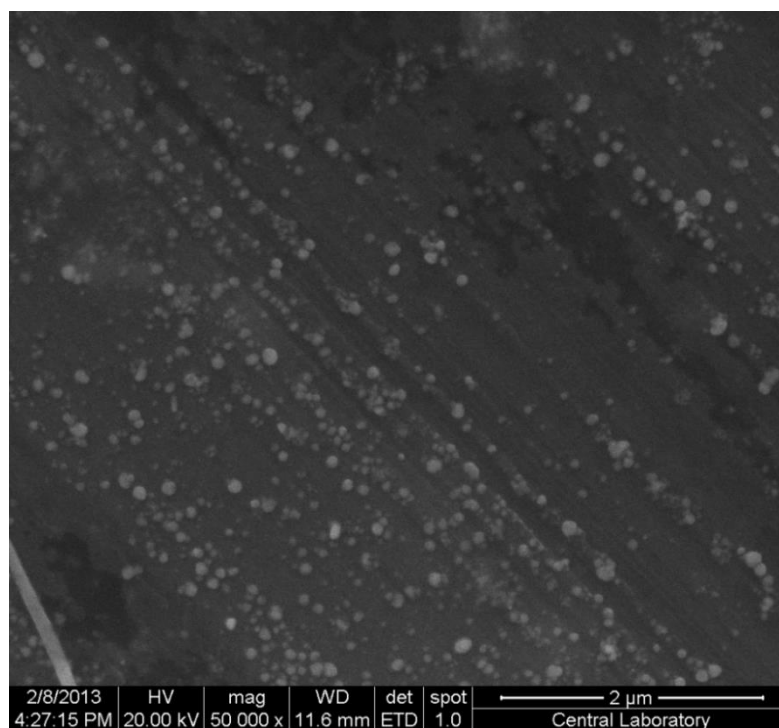


**Figure 32** SEM image of Ag NPs, experiment 16 in Table 3 (8mM AgNO<sub>3</sub>, 2 mM DA & 25 μM NaOH)

Lower NaOH concentration was also tried (10 μM) in experiments 15 and 17. SEM image (Figure 33) revealed large (>1 μm) linear and branched fibrillar structures with high aspect ratios. SEM micrographs also showed the formation of long and narrow individual fibers.

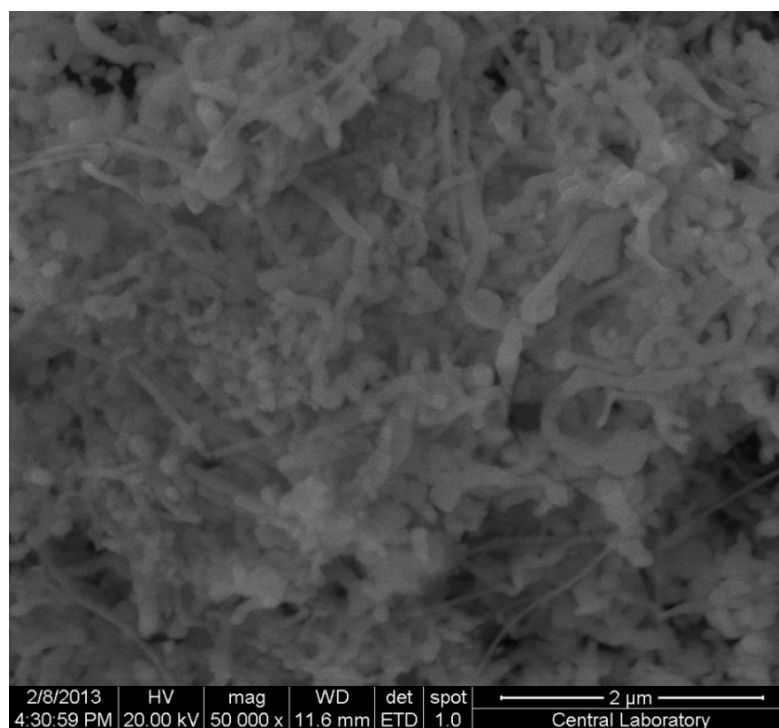


**Figure 33** SEM image of Ag NPs, experiment 15 in Table 3 (8mM AgNO<sub>3</sub>, 1 mM DA & 10 μM NaOH)

Herein, NaOH concentration had an important role in the formation of particles, again. In order to form NPs at mM concentrations of AgNO<sub>3</sub> and DA, NaOH concentration must be much lower than used with μM levels.

In addition, synthesis was tried when the medium didn't contain NaOH (Table 4 and Table 5). Excess amount of AgNO<sub>3</sub> was used. Experiment 19 and 20 resulted with dopamine-quinone formation (Figure 34) which turned into dopamine-chrome within 24 hours because the medium is neutral. Excessive AgNO<sub>3</sub> alone exhibited an oxidizing effect on dopamine but the mechanism didn't go further than dopamine-chrome form.

**Table 4** The summary of the experimental conditions in terms of the concentrations of the precursors (at millimolar level), without NaOH

Exp.	Conc. Of AgNO <sub>3</sub>	Conc. Of DA	Conc. Of NaOH
19	10.6 mM	2.7 mM	-
20	21.3 mM	2.7 mM	-

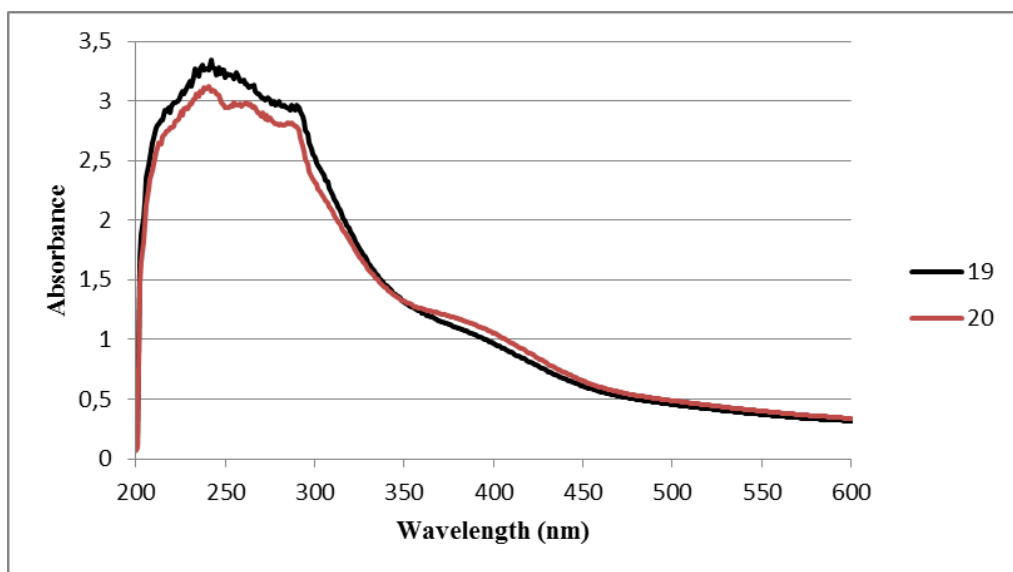


**Figure 34** UV-vis spectra of experiments 19 & 20

In trials 21, 22 and 23, yellow-colored solution with black particles were obtained. Supernatant was described as dopamine-quinone (Figure 35). Black precipitate was polydopamine (Jiang *et. al*, 2011). Too much oxidizing agent (20, 25 and 30 times excessive than DA) activated all steps leading to polymerization of dopamine.

**Table 5** The summary of the experimental conditions in terms of the concentrations of the precursors (at millimolar level), without NaOH

Exp.	Conc. Of AgNO <sub>3</sub>	Conc. Of DA	Conc. Of NaOH
21	42.6 mM	2.7 mM	-
22	53.3 mM	2.7 mM	-
23	66.6 mM	2.7 mM	-

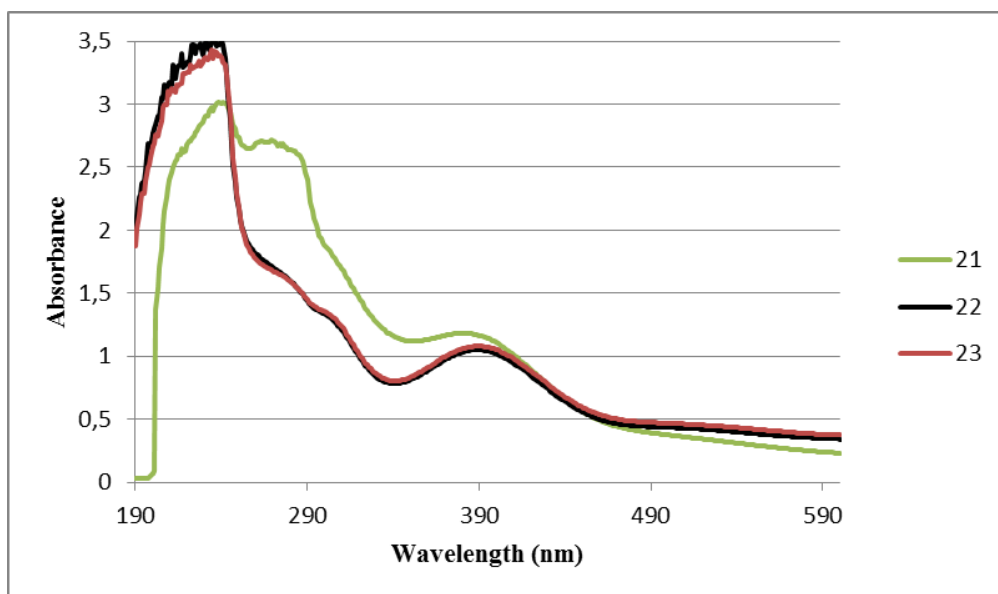


**Figure 35** UV-vis spectra of experiments 21, 22 & 23

### 3.3 Raman Spectroscopy Studies

SERS spectra of DA, DQ, DC, polydopamine on the surface of synthesized silver nanoparticles and the electrodeposited dopamine on the porous surface of silver electrode were obtained. During the SERS measurement of the DA, DQ and DC, citrate reduction prepared silver nanoparticles were used. Due to the temporary failure in the Raman Spectrometer in our laboratory, all related measurements were carried out at the METU Central Laboratory.

In our SERS studies we focused on the investigation of the bidentate silver catecholamine complex formation. Therefore, mainly the band at 1480-1490  $\text{cm}^{-1}$  range was searched in all SERS spectra. As mentioned before, it is used as the fingerprint for catecholamines (Table 6) since they are adsorbed to silver surface through metal-oxygen bonds (Lee *et al.*, 1988). It is attributed to the C=C phenyl stretch (McGlashen *et al.*, 1990). This band wasn't observed in the Raman spectrum of dopamine, expectedly (Figure 36).

bands	DA ( $\text{cm}^{-1}$ )
$\nu_{15}$	1152
$\nu_{\text{C-O}}$	1269
$\nu_3$	1331
$\nu_{19a}$	1424
$\nu_{19b}$	1479
$\nu_{8a}$	1572
$\nu_{8b}$	1584

**Table 6** Raman bands of DA (Lee *et al.*, 1988)

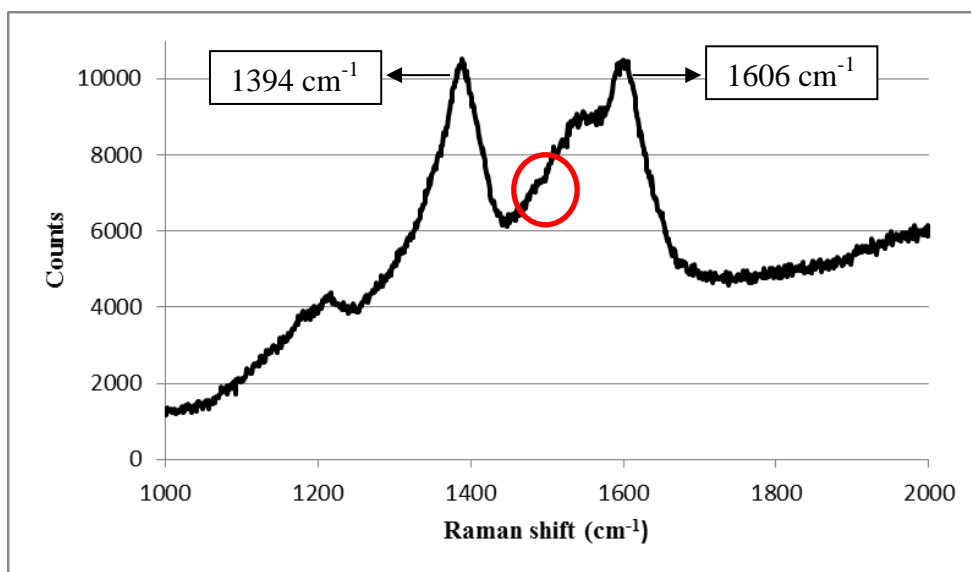


**Figure 36** Surface-enhanced Raman spectrum of  $10^{-3}$  M DA solution

On the contrary, DA functionalized Ag NPs displayed  $1493\text{ cm}^{-1}$  band (Figure 37) which may prove the dopamine oxidation on the silver surface during nanoparticle formation.

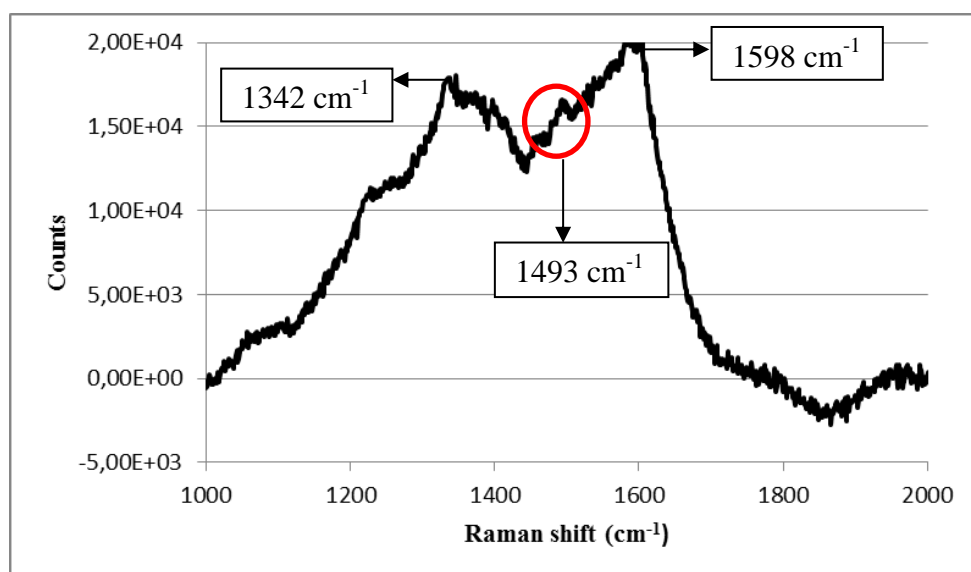


**Figure 37** Raman spectrum of polydopamine on the surface of synthesized Ag NPs

After electrolysis of dopamine in pH 7  $\text{KClO}_4$  with Ag electrode, roughened surface of electrode was investigated by Raman Spectrometer. Expected stretch was appeared at  $1480\text{ cm}^{-1}$  as a weak band (Figure 38). Although it was difficult to differentiate it as a peak, it might be a sign of the achievement of desired structure and accumulation on the surface of electrode. It is predicted that during electron

transfer, dopamine reacts with silver by bonding to surface through bidentate complex formation.  $1600\text{ cm}^{-1}$  band was appeared in all of spectra displayed here, which belongs to  $\text{NH}_2$  stretch.

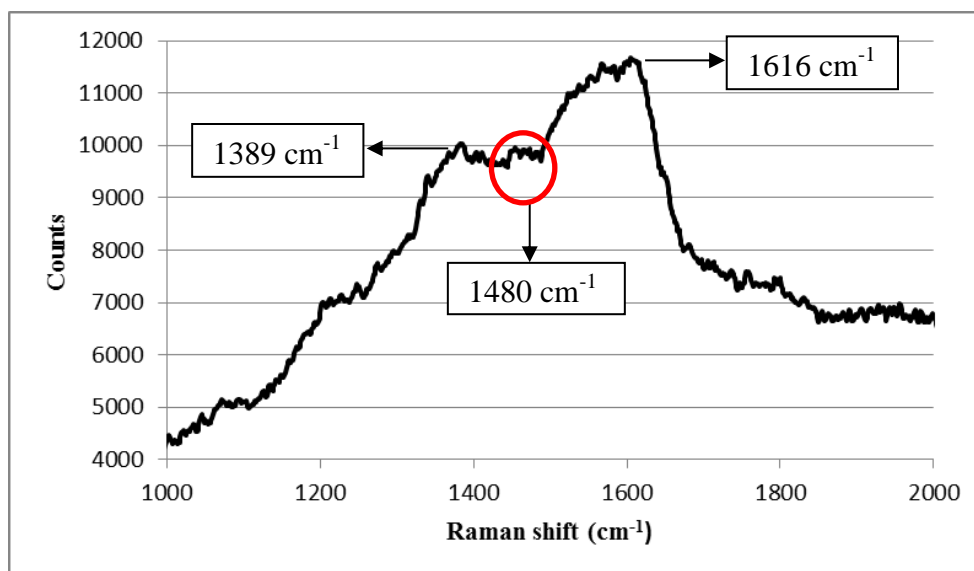


**Figure 38** Surface-enhanced Raman spectrum of silver electrode surface after electrolysis of dopamine in pH 7  $\text{KClO}_4$



## CHAPTER 4

### CONCLUSION

In this study, oxidation characteristic of dopamine was focused. Dopamine-ketone forms were obtained on the surface of silver electrode and silver nanoparticles. Silver electrodes were used for the electrolysis of dopamine. Electrode surface, oxidation products and nanoparticles were determined with UV-vis and Raman Spectrometry. Surface-enhanced Raman spectrum of dopamine didn't exhibit the catecholamine characteristic band  $1480\text{ cm}^{-1}$ . However, it was observed as a weak band in the spectrum of silver electrode surface. Even though it was difficult to describe it as a peak, it might be promising evidence about this thesis' starting point.

Dopamine functionalized silver nanoparticles were synthesized simply; with silver nitrate, dopamine and NaOH. While dopamine was oxidized, silver was reduced to silver nanoparticles. During the process, dopamine was attached to the surface of silver nanoparticles in the polydopamine form. These particles were characterized by UV-vis Spectroscopy, Raman Spectroscopy, SEM and TEM. In the Raman spectrum of DA functionalized Ag nanoparticles, expected at  $1493\text{ cm}^{-1}$  band was appeared. This appearance pointed that predicted structure was obtained on the surface of synthesized silver nanoparticles.

TEM and SEM images revealed the importance of oxidant concentration and amount of NaOH in the medium. When particles were synthesized with  $\mu\text{M}$  concentrations of  $\text{AgNO}_3$  and DA, NaOH concentration has a determining effect. When  $250\text{ }\mu\text{M}$  NaOH was used, nanoparticles didn't form.  $1\text{mM}$  was the optimum concentration. In addition, adding excess amount of  $\text{AgNO}_3$  speeds up the formation and smaller particle size was achieved. On the other hand, when particles were synthesized with  $\text{mM}$  concentrations of  $\text{AgNO}_3$  and DA, two different situations occurred. Firstly, high concentrations of NaOH showed a polymerizing effect. This is because, at high concentrations of  $\text{AgNO}_3$  and DA, oxidation occurs more readily. Adding NaOH accelerates the process and it continues to the formation of polydopamine. In the other case, low concentration of NaOH facilitated the formation of dopamine functionalized silver nanoparticles. However, this time they had larger size compared to the particles synthesized with  $\mu\text{M}$  concentrations of  $\text{AgNO}_3$  and DA. Again, smaller particles were obtained when excess amount of  $\text{AgNO}_3$  was increased. When  $\text{AgNO}_3$  to DA ratio was 4; particle size was  $75\text{ nm}$  as average. However, it was  $50\text{ nm}$  when ratio was 8. These nanoparticles were formed by using  $25\text{ }\mu\text{M}$  of NaOH. Particle dispersion was not clear when  $10\text{ }\mu\text{M}$  of NaOH was used. The conditions which didn't contain NaOH in the medium revealed the oxidizing power of  $\text{AgNO}_3$ . Increments in the excess amount of it led to polydopamine formation as can be expected.

## REFERENCES

- Bagotsky, S.V. (2006). *Fundamentals of Electrochemistry*.
- Bard, A.J. (1963). High Speed Controlled Potential Coulometry. *Anal. Chem.*, 35, 9, 1125-1128.
- Bisaglia, M., Mammi, S., & Bubacco, L. (2007). Kinetic and Structural Analysis of the Early Oxidation Products of Dopamine Analysis of the Interactions With  $\alpha$ -Synuclein. *J. Biol. Chem.*, 282, 21, 15597–15605.
- Borovansky, J., Edge, R., Land, E., Navaratnam, S., Pavel, S., Ramsden, C., Riley, P., & Smit, N. (2006). Mechanistic Studies of Melanogenesis: the Influence of N-Substitution on Dopamine Quinone Cyclization. *Pigm. Cell. Res.*, 19, 170–178.
- Cao, G., (2004). *Nanostructures and Nanomaterials*.
- Corona-Avendano, S., Alarcon-Angeles, G., Ramirez-Silva, M. T., Rosquete-Pina, G., Romero-Romo, M., & Palomar-Pardave, M. (2007). On the Electrochemistry of Dopamine in Aqueous Solution. Part I: The Role of [SDS] on the Voltammetric Behavior of Dopamine on a Carbon Paste Electrode. *J. Electroanal. Chem.*, 609, 17-26.
- Entschladen, F., Lang, K., Drell, L. T., Joseph, J., & Zaenker, K.S. (2002). Neurotransmitters Are Regulators for the Migration of Tumor Cells and Leukocytes. *Cancer Immunol. Immun.*, 51, 9, 467-482.
- Evanoff, D., & Chumanov, G. (2005). Synthesis and Optical Properties of Silver Nanoparticles and Arrays. *ChemPhysChem.*, 6, 1221-1231.
- Ferrari, M. (2005). Cancer Nanotechnology: Opportunities and Challenges. *Nat. Rev. Cancer*, 5, 161-171.
- Fleischmann, M., Hendra, P.J., & McQuillan, A. J. (1974). Raman Spectra of Pyridine Adsorbed at a Silver Electrode. *Chem. Phys. Lett.*, 26, 163-166.
- Glaspell, P.G., Zuo, C., & Jagodzinski, P. W. (2005). Surface Enhanced Raman Spectroscopy Using Silver Nanoparticles: The Effects of Particle Size and Halide Ions on Aggregation. *J. Clust. Sci.*, 6, 1, 39-51.
- Hornykiewicz, O. (2002). Dopamine Miracle: From Brain Homogenate to Dopamine Replacement. *Movement Disord.*, 7, 3, 501-508.
- Kerry, N. & Rice-Evans, C. (1999). Inhibition of Peroxynitrite-Mediated Oxidation of Dopamine by Flavonoid and Phenolic Antioxidants and Their Structural Relationships. *J. Neurochem.*, 73, 1, 247-253.
- Kissinger, P.T., & Heineman, W.R. (1983). Cyclic Voltammetry. *Journal of Chem. Educ.*, 60, 9, 702-706.
- Kneipp, K., Kneipp, H., Itzkan, I., Dasari, R., & Feld, S. (1999). Ultrasensitive Chemical Analysis by Raman Spectroscopy. *Chem. Rev.*, 99, 2957-2975.
- Lee, P.C., & Meisel, D. (1982). Adsorption and Surface-Enhanced Raman of Dyes on Silver and Gold Sols. *J. Phys. Chem.*, 86, 3391-3395.

- Lee, S.N., Hsieh, Z.Y., Paisley, F.R., & Morris, D.M. (1988). Surface-Enhanced Raman Spectroscopy of the Catecholamine Neurotransmitters and Related Compounds. *Anal. Chem.*, 60, 442-446.
- Lin-Zhang, S. (2012). *Raman Spectroscopy and its Application in Nanostructures*.
- Ma, Y., Niu, H., Zhang, Y., Cai, Y. (2011). One-step Synthesis of Silver/Dopamine Nanoparticles and Visual Detection of Melamine in Raw Milk. *Analyst*, 136, 4192-4196.
- McGlashen, M.L, Davis, K.L., & Morris, M.D (1990). Surface-Enhanced Raman Scattering of Dopamine at Polymer-Coated Silver Electrodes. *Anal. Chem.*, 62, 846-849.
- Miyazaki, I., & Asanuma, M. (2009). Approaches to Prevent Dopamine Quinone-Induced Neurotoxicity. *Neurochem. Res.*, 34, 698-706.
- Mnyusiwalla, A., Daar, S. A., & Singer, A.P. (2003). Mind the gap: Science and Ethics in Nanotechnology. *Nanotechnology*, 14, R9-R13.
- Napolitano, A., Crescenzi, O., Pezzella, A., & Prota, G. (1995) Generation of the Neurotoxin 6-Hydroxydopamine by Peroxidase/ H<sub>2</sub>O<sub>2</sub> Oxidation of Dopamine. *J. Med. Chem.*, 38, 917-922.
- Panacek, A., Kvitek, L., Prucek, R., Kolar, M., Vecerova, R., Pizurova, N., Sharma K.V., Nevecna, T., & Zboril, R. (2006). Silver Colloid Nanoparticles: Synthesis, Characterization, and Their Antibacterial Activity. *J. Phys. Chem., B*, 110, 16248-16253.
- Postma, A., Yan, Y., Wang, Y., Zelikin, A. N., Tjipto, E., & Caruso, F. (2009). Self-Polymerization of Dopamine as a Versatile and Robust Technique to Prepare Polymer Capsules. *Chem. Mater.*, 21, 3042-3044.
- Raman, C.V. (1928). A New Radiation. *Indian J. Phys.*, 2, 387-398.
- Selvaraju, T., & Ramaraj, R. (2003). Simultaneous Determination of Dopamine and Serotonin in the Presence of Ascorbic Acid and Uric Acid at Poly(o-phenylenediamine) Modified Electrode. *J. Appl. Electrochem.*, 33, 759-762.
- Shervedani, R. K., & Alinajafi-Najafabadi, H. A. (2011). Electrochemical Determination of Dopamine on a Glassy Carbon Electrode Modified by Using Nanostructure Ruthenium Oxide Hexacyanoferrate/Ruthenium Hexacyanoferrate Thin Film. *Int. J. Electrochem.*, 2011, 1-11.
- Song, C. K., Lee, S. M., Park, T. S., & Lee, B. S. (2009) Preparation of Colloidal Silver Nanoparticles by Chemical Reduction Method. *Korean J. Chem. Eng.*, 26(1), 153-155.
- Sun, W., Yang, M. & Jiao, K. (2007). Electrocatalytic Oxidation of Dopamine at an Ionic Liquid Modified Carbon Paste Electrode and Its Analytical Application. *Anal. Bioanal. Chem.*, 389, 1283-1291.
- Starowicz, M., Stypula, B., & Banas, J. (2006). Electrochemical Synthesis of Silver Nanoparticles. *Electrochem. Commun.*, 8, 227-230.
- Stokes, A. H., Hastings, T.G., & Vrana, K.E. (1999). Cytotoxic and Genotoxic Potential of Dopamine. *J. Neurosci. Res.*, 55, 659-665.
- Tse, D. C. S., McCreery, R. L., & Adams, N. R. (1976). Potential Oxidative Pathways of Brain Catecholamines. *J. Med. Chem.*, 19, 1, 37-40.

Venton, B. J. & Wightman, M. R. (2003). Psychoanalytical Electrochemistry: Dopamine and Behavior. *Anal. Chem.*, 414A-421A.

Vo-Dinh, T. (1998). Surface-enhanced Raman Spectroscopy Using Metallic Nanostructures. *Trend. Anal. Chem.*, 17, 8+9, 557-582.

Wang, J. (2005). Nanomaterial-Based Electrochemical Biosensors. *Analyst*, 130, 421-426.

Wei, Q., Zhang, F., Li, J., Li, B., & Zhao, C. (2010). Oxidant-induced Dopamine Polymerization for Multifunctional Coatings. *Polym. Chem.*, 1, 1430-1433.

West, J. L. & Halas, N. J. (2003). Engineered Nanomaterials for Biophotonics Applications: Improving Sensing, Imaging, and Therapeutics. *Annu. Rev. Biomed. Eng.*, 5, 285-92.

Young, T. A. (1981). Rayleigh Scattering. *Appl. Optics.*, 20, 4, 533-535.